Hybridization of PolyJet and Direct Write for the Direct Manufacture of Functional Electronics in Additively Manufactured Components

Kevin Blake Perez

Thesis submitted to the faculty of the Virginia Polytechnic Institute and State University in partial fulfillment of the requirements for the degree of

Master of Science
In
Mechanical Engineering

Christopher B. Williams (Chair)
Jan Helge Bøhn
Kathleen Meehan

December 18, 2013
Blacksburg, Virginia

Keywords: Additive Manufacturing, Direct Write, Printed Electronics, Conductive Ink, Component Embedding

Hybridization of PolyJet and Direct Write for the Direct Manufacture of Functional Electronics in Additively Manufactured Components

Kevin Blake Perez

ABSTRACT

The layer-by-layer nature of additive manufacturing (AM) allows for access to the entire build volume of a component during manufacture including the internal structure. Voids are accessible during the build process and allow for components to be embedded and sealed with subsequently printed layers. This process, in conjunction with direct write (DW) of conductive materials, enables the direct manufacture of parts featuring embedded electronics, including interconnects and sensors.

The scope of previous works in which DW and AM processes are combined has been limited to single material AM processes. The PolyJet process is assessed for hybridization with DW because of its multi-material capabilities. The PolyJet process is capable of simultaneously depositing different materials, including rigid and elastomeric photopolymers, which enables the design of flexible features such as membranes and joints. In this work, extrusion-based DW is integrated with PolyJet AM technology to explore opportunities for embedding conductive materials on rigid and elastomeric polymer substrates. Experiments are conducted to broaden the understanding of how silver-loaded conductive inks behave on PolyJet material surfaces.

Traces of DuPont 5021 conductive ink as small as 750μm wide and 28μm tall are deposited on VeroWhite+ and TangoBlack+ PolyJet material using a Nordson EFD high-precision fluid dispenser. Heated drying at 55°C is found to accelerate material drying with no significant effect on the conductor's geometry or conductivity. Contact angles of the conductive ink on PolyJet substrates are measured and exhibit a hydrophilic interaction, indicating good adhesion. Encapsulation is found to negatively impact conductivity of directly written conductors when compared to traces deposited on the surface. Strain sensing components are designed to demonstrate potential and future applications.

ACKNOWLEDGEMENTS

First and foremost, I would like to thank my family for their unwavering support throughout my educational endeavors.

I would also like to thank Dr. Jan Helge Bøhn and Dr. Kathleen Meehan for their guidance and help as participating members of my committee.

Research and Development funding is acknowledged from the Manufacturing and Industrial Technologies Division of the Air Force Research Laboratory Materials and Manufacturing Directorate.

The following authors are acknowledged for their previous work and illustrations, Palmer, Kataria, Williams, Stiltner, Li, Gibson, Goth, Robinson, Casanova, Sun, Castillo, Allen, Lopes, Breyfogle, Wang, and Cormier.

Support and guidance are critical to anyone's educational progress, but the DREAMS Lab has provided much more than that for me. I acknowledge my peers who have helped me through the day to day rigor of earning an advanced degree. Through coursework and research, they have guided me as things became daunting and overwhelming.

Finally, I would not be here if not for the patience and guidance of Dr. Christopher B. Williams. His enthusiasm and cultivation of a cooperative work environment in the DREAMS Lab has made my experience lasting and immensely valuable. I had the opportunity to listen to a presentation regarding the fundamental culture behind the Systems Realization Lab at Dr. Williams' alma mater Georgia Tech. There I learned the importance of creating a truly collaborative research environment among my fellow researchers and advisor. The results of this culture are inspiring. I hope that my efforts as a lab member have helped to cultivate a similar environment within the DREAMS Lab. Dr. Williams' support, criticism, and most of all, patience, is admired and appreciated.

TABLE OF CONTENTS

Table of Figures

Table of Tables

1 INTRODUCTION TO HYBRIDIZATION OF ADDITIVE MANUFACTURING AND DIRECT WRITE TECHNOLOGIES

The shape and form of traditionally manufactured goods are designed to accommodate the technologies available to create them. With computer numerical control (CNC) machining for example, jigs and fixtures are used to secure components while other tools mill away material where it is not needed. The material to be removed must be accessible from the external surface. Other manufacturing technologies have similar constraints. Because of the layer-wise additive manufacturing (AM) build process (detailed in Section 1.1), many of these constraints are eliminated or circumvented. Of particular interest is AM's ability to encapsulate components entirely during the build process. An illustration of how this is done with AM is shown in Figure 1.1. With traditional manufacturing, the cavities would need to be accessed from the component's external surface—preventing the complete encapsulation of the embedded component.

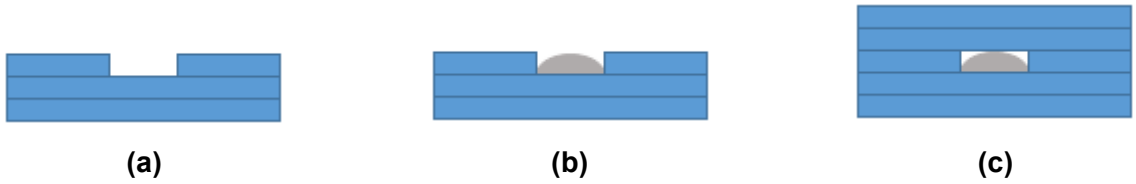

Figure 1.1: Illustration of the Additive Manufacturing component embedding process. (a) Print pausing step; (b) Embedding step; and (c) Print resuming step

The embedding process can be used to encapsulate various types of actuators and sensors. When considering actuation with traditional manufacturing, different types of joints are designed to afford degrees of freedom in motion. With AM, complex compliant geometries can be used instead to provide these degrees of freedom for actuation and movement. Furthermore, the PolyJet process specifically can create more complex compliant mechanisms by leveraging the technology's multi-material capabilities. PolyJet can combine both rigid and elastomeric polymers in a single build to create flexible articulated joints wherein sensors and actuators may be embedded (Section 1.2). These sensors could even provide feedback for closed-loop control of the embedded actuation system. The fabrication and embedding of the sensing components may be further facilitated by direct write (DW) technologies.

Direct write is a principal set of technologies that allows for the selective deposition of material (Section 1.3). By depositing conductive materials, written electrical interconnects on additively manufactured surfaces have been demonstrated [1]. These interconnects can also be directly written during the build process to create fully embedded and encapsulated conductors using the embedding process described in Figure 1.1 [2], [3]. Moreover, these conductive materials can also be purposed to create sensors. Resistive and capacitive sensors often rely on special geometric configurations of one or more conductors. These geometries, like the strain gage shown in Figure 1.2, can be digitally manufactured and embedded into additively manufactured components using direct write technology.

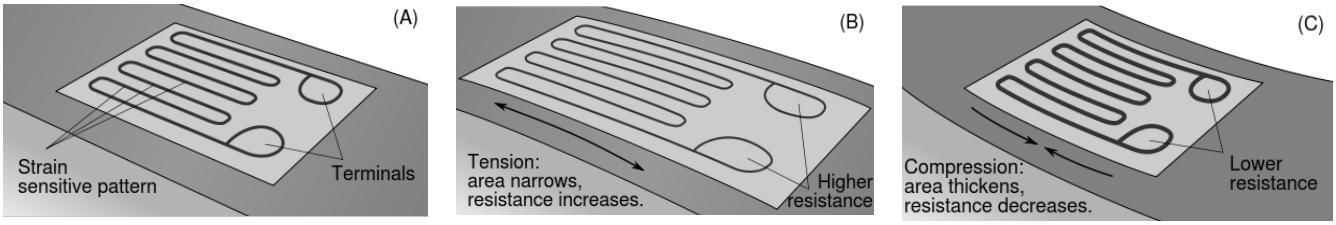

Figure 1.2: Illustration of the operating principles of a strain gage used under fair use, 2013 [4]

The combination of DW and PolyJet technologies has not been researched before in the literature (Section 2.1). By combining these two processes, one can directly manufacture complex, multi-material components that feature structurally integrated actuation and sensing in a single build. **The primary goal of this thesis is to develop a direct write system for depositing conductive materials during the PolyJet manufacturing process to create embedded and functional electronic interconnects and sensors**. A secondary goal is to characterize and assess the compatibility of the developed direct write system with PolyJet. Specifically, **research goals include gaining an understanding of (i) deposition geometry, (ii) material adhesion, and (iii) conductivity of the conductive material when deposited on the surface of different PolyJet substrates and when fully embedded** (Chapter 4).

The following sections give a brief overview of the PolyJet process, component embedding, and direct write to explain their working principles. Thereafter, the remainder of the thesis is outlined.

1.1 Additive Manufacturing

Additive manufacturing is unique in many ways and has allowed for creative avenues in manufacturing by leveraging its layer-by-layer nature. Fundamentally, AM begins with a 3-dimensional representation of a part in virtual space as an ".STL" file. The .STL file represents a solid body's surfaces using triangles, much like in digital animation. More triangles in an STL file often equate to higher resolution surfaces. Beyond the .STL file, but before manufacture, the specific AM technology will slice the .STL file into a sequence of layers to be built sequentially on top of one another. Again, more slices typically imply higher resolutions. Beyond this step, the methods of material patterning and manufacture differ from technology to technology. Each process may follow a different permutation of the additive manufacturing sub-functions presented in Figure 1.3. The figure is a morphological matrix proposed by Williams and coauthors that demonstrates the different potential working principles of AM processes [5]. The work herein focuses specifically on the use of PolyJet AM technology (indicated by the dotted path in Figure 1.3); other AM technologies are discussed in detail by Gibson, Rosen, and Stucker [6].

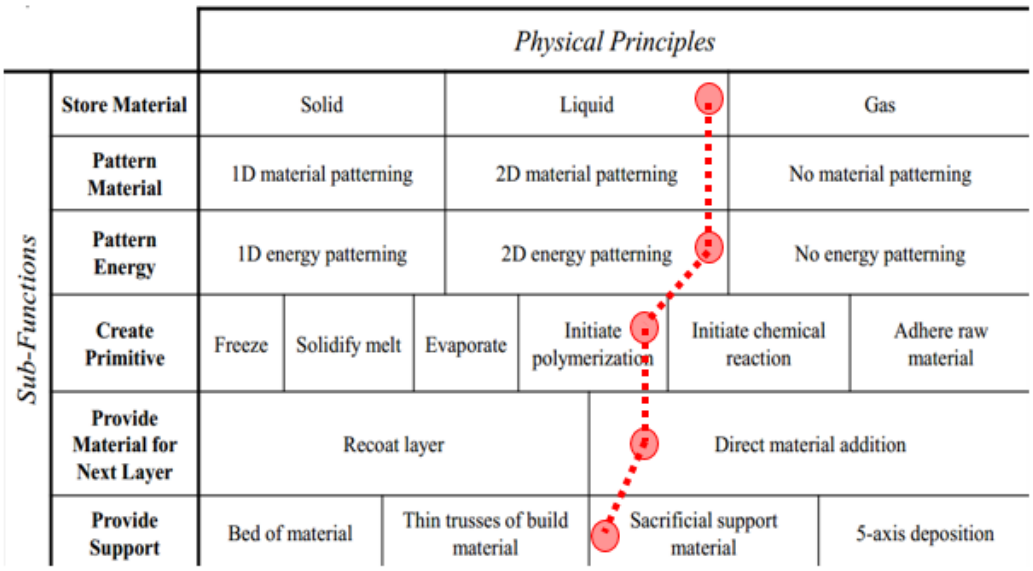

Figure 1.3: Morphological matrix of additive manufacturing sub-functions [5]**. The PolyJet's sub-functions are indicated by the dotted path used under fair use, 2013.**

PolyJet is a material jetting AM process that selectively patterns liquid photopolymer using drop-on-demand inkjet technology. The photopolymer is cured on the part surface by scanning

UV lamps as the material is deposited. The slices of the desired STL file are transformed into bitmap images. The printheads deposit material according to this bitmap image and the Z-direction thickness of the droplets give the layer dimension. For repeatability, a leveling roller passes over the layer to ensure the droplets are at a uniform layer height of 32 μm. This layer-based process is illustrated in Figure 1.4. This step is repeated many times until the full height of a part is realized. While the PolyJet process is capable of 16 μm layer thicknesses, this printing mode only allows for single material printing and is thus not considered.

The PolyJet's multiple print heads allow for multiple materials to be deposited in a single build including support and structural material. The support material is a gel-like photopolymer that can be washed away after a component is fully printed. There are many different commercially available photopolymers. This work uses VeroWhite+ and TangoBlack+ materials; VeroWhite+ is a white and rigid photopolymer, while TangoBlack+ is black in color and behaves much like an elastomer. Using both materials in a single component allows for rigid structures and flexible surfaces such as hinges, joints, or membranes. By designing voids and channels into these parts, it is also possible to embed foreign components during the build process as discussed in the following section.

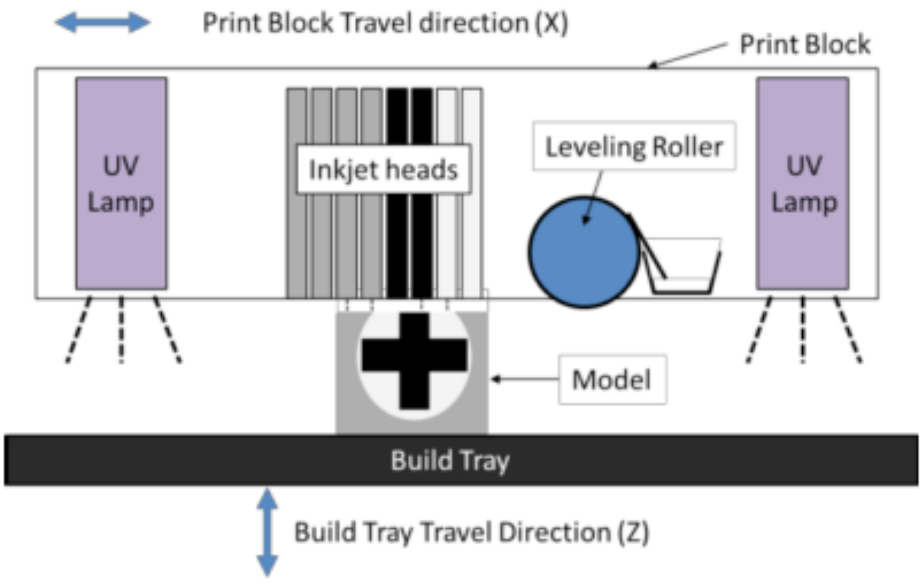

Figure 1.4: Stratasys Objet Connex350 print block schematic and building process used under fair use, 2013 [7]

1.2 Component Embedding

The layer-by-layer nature of AM allows access to the entire build volume of a component during manufacture including the internal structure. Leveraging this advantage, previous work has investigated the embedding of foreign components into additively manufactured parts [2], [8], [9]. Generally, the build process is paused midway through manufacture and components are placed into recesses or cavities below the build surface that have been designed into the 3D model. Sometimes inserts or 'shape converters' are made to cover the embedded component and create a flat surface on which to resume the build [2].

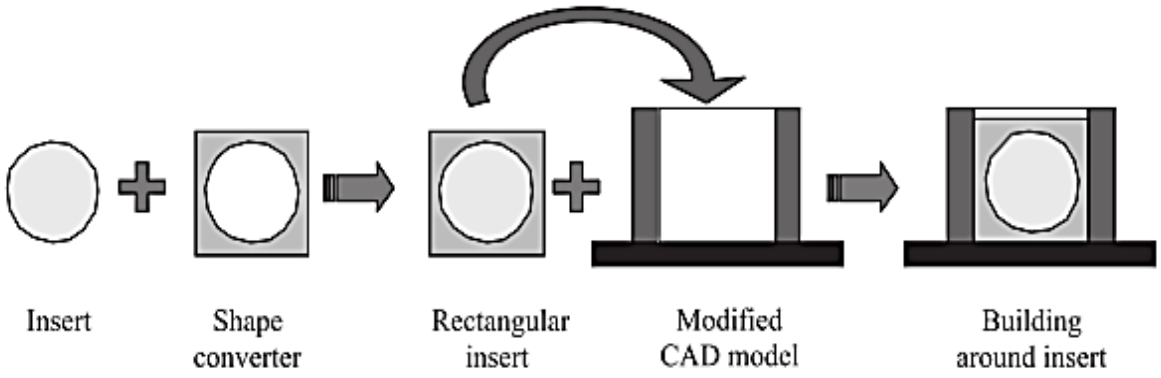

Figure 1.5: Generalized method for embedding components using shape converter used under fair use, 2013 [2]

Component embedding has been used to integrate electromechanical actuators such as motors [2]. Stiltner and coauthors demonstrated that fibers can also be used for actuation when embedded in PolyJet parts featuring multi-material compliant geometries, as shown in Figure 1.6 [8]. The compliant geometries are made possible by PolyJet's ability to print with multiple materials. Embedding components has numerous advantages including structural integration, weight savings, and fastener elimination. The next section discusses the advantages of direct-write technology in the context of component embedding with additive manufacturing.

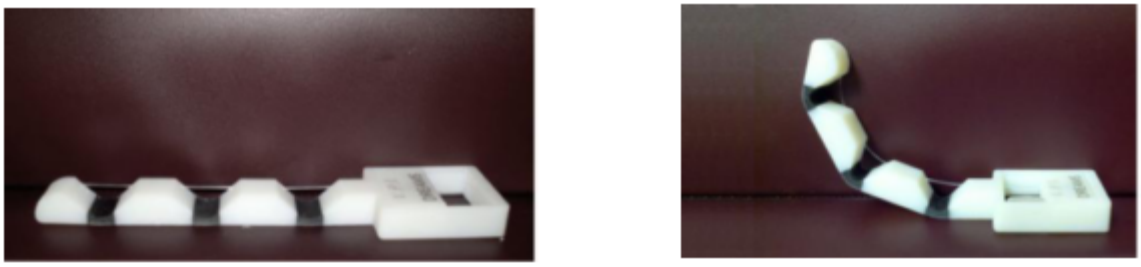

(a) As built **(b) Actuated**

Figure 1.6: Actuated finger example of fiber embedding for actuation of compliant geometries used under fair use, 2013 [8]

1.3 Direct Write of Circuits

Direct write technologies allow for depositing material selectively where needed. The technology is capable of single- and multi-layer, high-resolution, material deposition on both flat and conformal surfaces [10]. These technologies have been comprehensively reviewed [11]. Hon and coauthors' review includes methods capable of depositing nonconductive materials. However, the present work considers only DW methods for conductive materials because of the motivation to fabricate embedded electronics within additively manufactured components.

In general, DW processes have been researched and developed because of their potential to replace masked lithographic processes in electronics production for reducing waste, chemical usage as well as enabling non-planar and flexible substrates. For example, in a review of DW applications, Church and coauthors assert that DW enables rapid manufacturing of sensors and antennae because it eliminates the masking and etching steps of conventional electronics fabrication [12].

All DW technologies serve the same function (i.e., selective deposition of conductive traces); however, the means of realizing this primary design goal varies dramatically. The main categories of the technology are reviewed in Section 2.2 and include:

- **Extrusion** technologies that use positive pressure to extrude fluid materials through a small nozzle and onto a substrate.
- **Droplet jetting** technologies that eject small droplets of material onto a substrate.
- **Aerosol jetting** systems aerosolize a material to create a gaseous stream that is aerodynamically focused and deposited on the substrate.

- **Laser transfer** systems use a laser's energy to transfer material onto a substrate surface.
- **Tip transfer** deposition methods use capillary flow of an ink on microscale tip onto the substrate surface [11].

When combined with additive manufacturing processes, DW enables the creation of complex and conformal electronics that are structurally integrated into a manufactured part. These applications are detailed in Section 2.3, which reviews different combinations of additive and direct write manufacturing processes from previous works.

1.4 Thesis Roadmap

The PolyJet process provides novel avenues for development with embedding and multi-material capabilities when combined with direct write technology. A combination of the two technologies has not been previously documented in the literature. To qualify the hybridization of direct write technology with the PolyJet process, **a direct write system is developed for implementation within a Stratasys Objet350 Connex PolyJet printer. The interaction between the conductive direct write and PolyJet materials is investigated in this work, and is guided by fundamental research questions presented in Chapter 4.**

In Chapter 2, a review of previous instances of the combination of additive manufacturing and direct write technologies and their applications, is presented. The review explores DW in the context of the elements that make a particular DW technology compatible with additive manufacturing by examining the cost, resolution, and material capabilities. Chapter 2 closes with a discussion of the trends in rationale from previous work and potential challenges to hybridizing PolyJet and DW of conductive materials. These trends and roadblocks motivate the development of the research questions that guide the characterization of the resultant system.

Chapter 3 synthesizes information gained from the literature review and from a perceived customer needs analysis to design and embody a DW platform for depositing conductive materials onto PolyJet substrates during the build process. A systematic design methodology using quality function deployment is used to develop a fully embodied system. The final physical system is presented at the end of Chapter 3.

Using this system as a repeatable means for depositing conductive material, the research questions are addressed by experimentation, which is detailed in Chapter 4. This chapter is subdivided into four main sub-sections, each concerning a different research question. The research questions serve to bridge the research gaps discussed in Chapter 2 by characterizing the quality and functionality of the directly written conductive elements. Specifically, the four research questions investigate:

(i) Effects of DW process parameters on deposition resolution
(ii) Effects of heat-assisted conductive material drying
(iii) Adhesion characteristics of the conductive materials to the PolyJet substrates
(iv) Effects of encapsulation on the electrical performance of conductive materials

The conclusions of each experiment are discussed in each sub-section; however, a synthesis of the conclusions from the four experiments is withheld until Chapter 5 where conclusions on the overarching primary and secondary research goals are discussed.

Conclusions are offered in Chapter 5 along with a discussion regarding the potential of DW with the PolyJet process. Conclusions on the research goals of developing and qualifying a direct write system for the PolyJet process to create functional electronics are synthesized from the literature, machine design, and characterization sections (Chapters 2, 3, and 4). Conclusions on the secondary research goal of understanding the characteristics of the conductive materials on the PolyJet substrate are made primarily from the literature review and the research questions investigated in Chapter 4.

2 REVIEW OF DIRECT WRITE FOR ADDITIVE MANUFACTURING

Previous works have investigated different combinations of additive manufacturing and direct write technologies. However, before reviewing these applications, it is important to understand the conductive materials and the direct write technologies capable of dispensing them. The information gained from this review is then used in conjunction with a customer needs analysis to select the type of material and direct write technology to use with the PolyJet process (Chapter 3).

2.1 Conductive Direct Write Materials

Depositable conductive materials have found many industrial uses, especially in the manufacture of consumer electronics. Most depositable conductive materials or inks are composed of a conductive additive suspended in a fluidizing solvent. The solvent is often volatile so that it evaporates once deposited. Beyond these two main components, there are other additives to promote adhesion as well as to disperse the conductive constituents. The following subsections discuss the ink formulation, conductive capabilities and cost in that order. The final paragraph summarizes the relative advantages and disadvantages of the particular ink.

2.1.1 Metal-Loaded Inks

Metal-loaded (ML) inks are composed of metal microparticles and a volatile solvent. The solvent serves to fluidize the metal particles but evaporates after deposition. These inks are commercially used in large-scale screen printing of electrical interconnects on products such as LCD screens and solar panels.

The formulation of these inks is important, affecting ease of deposition and conductivity. As deposited, metal-loaded inks are shown to exhibit conductivities on the order magnitude of 10^5 S/m [13]. By weight, metal loadings of 30-75 percent by weight are common. Formulations with lower loadings are less viscous; however, they are also less conductive. The electrical path through deposited inks relies on particle-to-particle contact and interfaces, therefore higher metal loadings imply a higher particle density, more inter-particle contact, and thus a higher conductivity. Conductivity is often improved by heating the deposited features so that particles

actually sinter together at their contact sites. [13]. If the materials can be exposed to higher temperatures to undergo sintering, the conductivity approaches 10^7 S/m, the conductivity of bulk metals. This process is further detailed in Section 2.4.1.

The metals most commonly used are silver and gold because of their resistance to oxidation; however, this can be cost prohibitive (e.g. 70% silver by weight inks can cost about $2 USD per gram). Other formulations use metal particles suspended in a semi-conductive matrix (e.g. Malone and coauthors [14]). However, these materials are two orders of magnitude less conductive than bulk metals because of the low density of metal particles.

Of the three types of inks discussed in this work, metal-loaded inks are the most expensive and viscous. However, they are readily and widely available because of their applications in commercial electronic manufacturing. Moreover, they have a high metal content by weight percent, which theoretically results in a less porous conductor and overall higher conductivity.

2.1.2 Carbon-Loaded Inks

Carbon-loaded inks are similar in formulation to the metal-loaded inks discussed in the previous section, however with carbon as the conductive constituent. Once deposited, a fluidizing solvent evaporates and leaves behind conductive carbon traces. Carbon additives are also sometimes dispersed into paints or polymers and used in electromagnetic shielding or electrostatic dissipation applications.

When compared to metal-loaded inks, carbon inks have a lower conductivity by up to two orders of magnitude (10^3 S/m), as shown by Leigh and coauthors [15]. However, they reach this level of conductivity at about 32 percent by weight [16] and without high temperature processing. Because of the small size of the carbon constituents however, they can be difficult to disperse within the carrying fluid.

The carbon additives used include carbon microparticles, nanoparticles and nanotubes, which are suspended in a volatile fluidizing solvent. Carbon-based conductors may find applications in contexts where cost may be more critical than electrical performance as they cost less than $0.50 USD per gram. Their low cost and low conductivity influences their use in the aforementioned shielding and dissipative applications.

In summary, carbon-loaded materials are inexpensive but not nearly as conductive as their metal counterparts, which makes functional electronics less feasible. The small size of the conductive constituents makes them hard to disperse for homogeneous mixtures in carrier material. However, their low cost makes carbon based inks attractive when high conductivity is not required.

2.1.3 Metal-Organic Decomposition (MOD) Inks

Metal-organic decomposition (MOD) inks rely on a chemical reaction to produce metals conductors on a substrate surface. Metal-organic compounds are organic compounds that contain a metal atom bound to a carbon atom. The metals are dissolved in solvent such as toluene or xylene [17]. Because the metal atoms form stable bonds with other organic matter, the metals do not precipitate out or agglomerate.

Unreacted MOD inks have no particle loading. When exposed to a catalyst, the reaction that occurs causes conductive metals to precipitate. The catalyst can be a separate chemical compound or sometimes air. Air is a convenient catalyst, although special care has to be taken to ensure that the ink is stored under vacuum so that the reaction does not occur prematurely. MOD inks typically have a metal content of 20-25% by weight, which results in lower conductivity in comparison to metal-loaded inks (which have 60-70% metal content by weight). As with any metal ink, post-process sintering near the material's melting point can dramatically improve conductivity to nearing 10^7 S/m (the conductivity of bulk metals) [13].

MOD inks are comparable to metal-loaded inks as the cost is largely tied to the price of the conductor used (silver, gold, and copper). Again, silver and gold are primarily used because of their aversion to oxidation. Chemical processing steps for formulating MOD inks may also affect cost.

The reaction time for the metals to precipitate from MOD inks can also be longer than the dry times of solvent-based inks. It is also difficult to include binders to aid the adhesion of metal particles to the substrate. In a sintered state, conductivities should be comparable to metal-loaded inks that have also been sintered. However unsintered, the inks may be less conductive because of the lower metal loading and resulting high porosity and fewer contact surfaces for particle-to-particle conduction. Because the metal atoms form stable bonds with other organic

matter in an unreacted state, the metals do not precipitate out or agglomerate. Therefore, the inks have no particle loading, allowing their rheology to be tailored to the different deposition processes discussed in the following section.

2.2 Direct Write Technologies

In order for direct write technologies to integrate with AM processes, it is paramount that the material deposition system is maneuverable and reliably positioned. Additionally, for manufacturing relevance, the write speeds should be comparable to the corresponding AM process. While Hon and coauthors have comprehensively reviewed available direct write technologies [11], Aerosol Jet, inkjet, and extrusion methods are considered immediately relevant for hybridization with additive manufacturing since they afford freeform control of both the deposition tool and the material delivery system. Basic performance capabilities of these direct write technologies are summarized in Table 2.1 and the following sub-sections.

Table 2.1: Comparison of direct write technology capabilities. Adapted from [11]

Technology	Minimum Resolution	Viscosity Range	Max Write Speed
Inkjet	≥20 μm	≤0.1 Pa·s	0.30 mm^3/s
Aerosol Jet	≥10 μm	Not Applicable	0.25 mm^3/s
Extrusion	≥25 μm	≤5000 Pa·s	300 mm/s

Other direct write technologies discussed by Hon include laser- and tip-based transfer methods. However, they are excluded from this review due to their slow write speeds, incompatible reaction environments, large deposition tool heads, and/or material precursors that would be difficult to integrate with the PolyJet process. As both direct write and additive manufacturing technologies evolve, the excluded direct write processes may become relevant in the context of hybridization. The other technologies are sufficiently explained and analyzed in previous reviews of direct write technologies [11], [18].

2.2.1 Extrusion-Based Direct Write

Extrusion-based direct write deposition uses positive pressure to dispense conductive materials in fluid form through a small nozzle. Both syringe (Figure 2.1a) and micro-dispensing pump (Figure 2.1b) systems fall in this category. The pneumatic control of these systems allows

for dynamic operation and pressure regulation. Maintaining precise control over pressure is important as pressure directly affects feature width, even if ink type and nozzle diameter are held constant. These systems can also apply a vacuum to draw fluid into the dispense tip and mitigate dripping or over dispensing. The distance from which material can be deposited from the substrate can vary; however, it is understood that for different machine parameters (e.g., tool speed, material type, pressure) the dispensing height is important, especially as feature sizes become very small [13], [19].

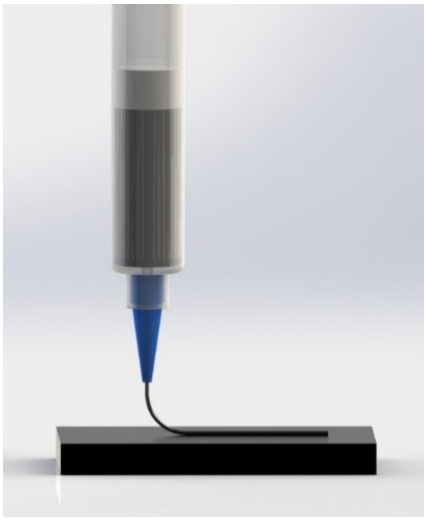

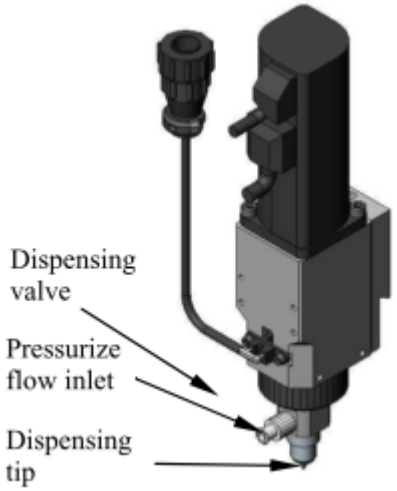

(a) **(b)**

Figure 2.1 – (a) schematic of basic syringe system (b) micro-dispensing pump used under fair use, 2013 [19]

Extrusions systems can dispense fluidized materials with viscosities up to 5000 Pa·s and can achieve feature widths as small as 25 μm. Linear writing speeds can reach 300 mm/s, although 50 mm/s is typically observed [11]. Volumetric rates depend on nozzle size, which is limited by the material selection.

Extrusion technologies are capable of dispensing heavily loaded conductive inks. Higher loadings results in higher particle density as-deposited and, thus results in, better conductivity. However, inks with high metal loadings are more viscous and can be difficult to dispense. Viscous inks require more pressure to dispense and the high particle content leads to clogging in the dispensing orifice. Using larger nozzle tip diameters alleviates clogging, although this negatively impacts the minimum achievable feature size of the system. Most importantly, high metal loadings improve conductivity but limit the minimum achievable feature size. Ideal inks balance loading for clog-free dispensing and desired feature resolution while maximizing conductivity.

Extrusion processes are favored for dispensing heavily loaded inks since they are capable of extruding such viscous material. Previous works have used inks with metal loadings in the 60-70% range [3], [9], [20], [21]. From a control perspective, extrusion systems are favorable for integration with AM technologies because the tool tip is maneuverable, can dispense in different orientations, and can process high volumes of material. Additionally, the 50 μm feature resolution is comparable to the PolyJet process (42 μm), although this resolution value may increase with the use of heavily-loaded inks.

2.2.2 Inkjet Direct Write

Similar to the technology in common inkjet printers, inkjet direct write is a droplet-based technology that places material where it is needed. Some inkjet direct write systems use a piezoelectric diaphragm and a small orifice to dispense material in liquid form. As the diaphragm expands, it places positive pressure on the fluid, which is expelled through the orifice as shown in Figure 2.2. Alternatively, some systems use a heat source to heat the ink and generate a bubble. This bubble provides the pressure to expel the droplet through the orifice. These heat-based jetting systems however, can cause solvents in an ink to volatize rapidly, leaving metal particles behind in the jetting chamber, which can clog the printing orifice.

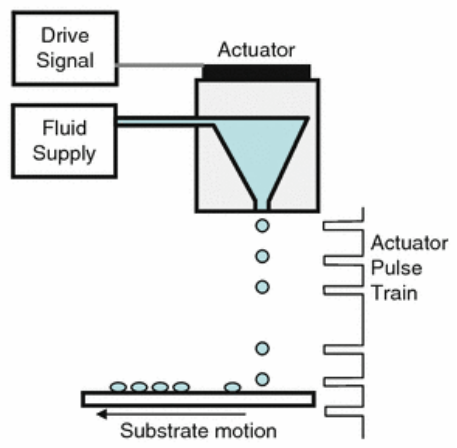

Figure 2.2 – Schematic of ink jet deposition used under fair use, 2013 [6], [22]

Inkjet systems can dispense fluid materials up to 100 mPa·s and can create features as small as 20 μm, which is significantly better than extrusion). The volumetric dispense rate of a single nozzle is only 0.3 mm^3/s; however, this can be increased by using an array of nozzles. The formation of droplets and their corresponding size is heavily influenced by the distance of a print head from the substrate [18]. Deviations from an optimal distance can result in poor resolution control. Unlike extrusion systems, inkjet technology has drop-by-drop control, which allows for more discrete placement of material.

Like extrusion technologies, inkjet systems can use metal or carbon loaded inks; however the inks must be less viscous to be compatible (i.e. lower solids loading) [18]. As with the extrusion-based systems, the particle loading plays a significant role in the dispense characteristics as well as conductivity. Higher concentrations imply higher conductivities; however, high concentrations make the ink more viscous and therefore difficult to jet. When compared to extrusion-based systems, for the same orifice diameter, inkjet systems are more sensitive to particle loading and clog at lower concentrations. A thorough review of droplet formation and viscosity limitations for ink jetting is found in [23].

Typical formulations of metal-loaded inks contain 30-40% metal by weight, although up to 50% loadings can be found [23]. These higher percent loadings requires? very small particle sizes that are susceptible to agglomeration, which can reduce jetting reliability [24]. Inkjet systems are also well suited for dispensing MOD inks as well. MOD inks' viscosities can be

tailored specifically for ink jetting [25]. Previous works have used multiple printing passes order to deposit more metal and improve conductivity.

Inkjet deposition heads are maneuverable and can also print in different orientations making them a good candidate for hybridization with AM. However, the offset distance between the substrate and print head is critical, requiring more sophisticated and precise motion control. Ink jetting can be tailored to produce traces with high resolution in arrays that are comparable to AM processes in terms of throughput. Compared to extrusion systems, ink jetting is capable of higher resolution. However, lower achievable metal loadings negatively impact conductivity.

2.2.3 Aerosol Jet direct write

Aerosol Jet direct write systems aerosolize solutions into a vapor stream to deposit material. For the direct write of conductive materials, metal- and carbon-loaded inks can be used. This mixture is dispensed through a high velocity nozzle as shown in Figure 2.3. The vapor accelerates through the nozzle and impacts the substrate surface. The aersolization process can help to dry out the solvent constituents of the solution and decrease dry times. The size distribution of the particles can be controlled independently of the feedstock's distribution using virtual impactors. A virtual impactor uses a secondary gas flow with a different flow rate. Smaller particles are diverted by the secondary flow. A larger particle's momentum prevents it from being diverted and continuing on the main path. This allows for a homogenous mixture of uniformly sized particles, which enables high resolution and consistent post-processing outcomes (discussed further in Section 2.4.1).

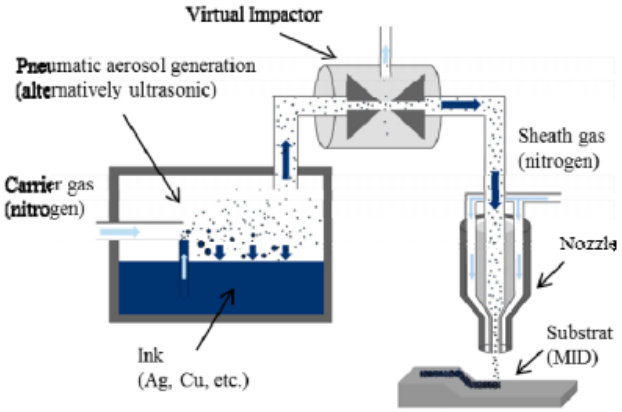

Figure 2.3 – Optomec Aerosol Jet process used under fair use, 2013 [26]

Aerosol Jet direct write is capable of producing features as small as 10 μm with linear write speeds of 300 mm/s although 50 mm/s is typically observed. Single passes can be as thick as 2 μm depending on the ink [27]. Therefore, at a resolution comparable to extrusion system (50 μm), the volumetric deposition rate is limited to 0.03mm^3/s. Although previous work has shown that it is possible to use multiple aerosol jets in parallel to increase throughput [28]. Because of the aersolization process, viscosity is not so much an issue as long as the material can be aerosolized (includes metal and carbon). However, the particle density of the material when deposited may not reflect the density of the bulk material after going through the aersolization process. The deposition head can also deposit material at a range of distances from the substrate surface. Deposition is possible with a standoff distance within the range of 1mm to 5mm [18]. This makes motion control for deposition on conformal surfaces simpler.

Again, the maneuverability of the deposition head and the systems control make Aerosol Jetting a good candidate for integration with additive manufacturing systems. The tolerance of the dispensing nozzle's standoff distance makes the system flexible and ideal for deposition on conformal surfaces. Flat surfaces or high volume production requirements however are better suited by the other technologies given the Aerosol Jet deposition rate is relatively low.

2.3 Previous Applications and Combinations of Additive Manufacturing and Direct Write of Conductive Materials

Given a detailed understanding of the different direct write technologies, previous work combining different direct write and additive manufacturing are presented. The works are listed chronologically in Table 2.2 and grouped according to their applications, which include:

- Electrical interconnects
- Discreet electronics
- Embedded antennae
- Battery fabrication
- Conformal electronics

The conclusion of this section discusses the trends identified in these works and the supporting rationale.

Table 2.2: Previously explored combinations of direct write and additive manufacturing

Author	Application	Direct Write Technology	Additive Technology	Year
Palmer	Interconnects	Micropump	Stereolithography	2004
Medina	Discreet Electronics	Pneumatic Extrusion	Stereolithography	2005
Robinson	Interconnects	Pneumatic Extrusion	Ultrasonic Consolidation	2006
Malone	Batteries	Mechanical Screw Extrusion	Mechanical Screw Extrusion	2008
Castillo	Conformal Electronics	Manual	Stereolithography	2009
Breyfogle	Antenna & Interconnects	Aerosol Jet	Fused Filament Fabrication	2013
Folgar	Interconnects	Aerosol Jet & Micropump	Selective Laser Sintering	2013

2.3.1 Electrical Interconnects

In 2004, Palmer and coauthors produced electrical interconnects between embedded electronic components using DW and stereolithography (SL) as the first example of combining AM with DW technology [1]. An nScrypt™ 3De micropump was used to directly write Heraeus PC 5915 metal-loaded silver ink on DSM Somos Corp ProtoTool™ photopolymer resin. The team manufactured the housing and embedded prefabricated electrical connectors. Interconnects between the connectors were directly written on the surface in a separate process. The ProtoTool™ resin was used because of its temperature resilience with a glass transition temperature of 100°C. The high transition temperature is desired to withstand the supplier's annealing recommendations for the metal-loaded inks. Discoloration of the ProtoTool™ material was reported when annealing at 120°C. Their work demonstrates how directly written interconnects can eliminate the need for cabling to reduce size and weight as shown in Figure 2.4. A 20 cm long trace of the material was measured to have a resistance of 3.6 Ohms,, which is 18 times more resistive than a comparable length of AWG 26-gage copper wire.

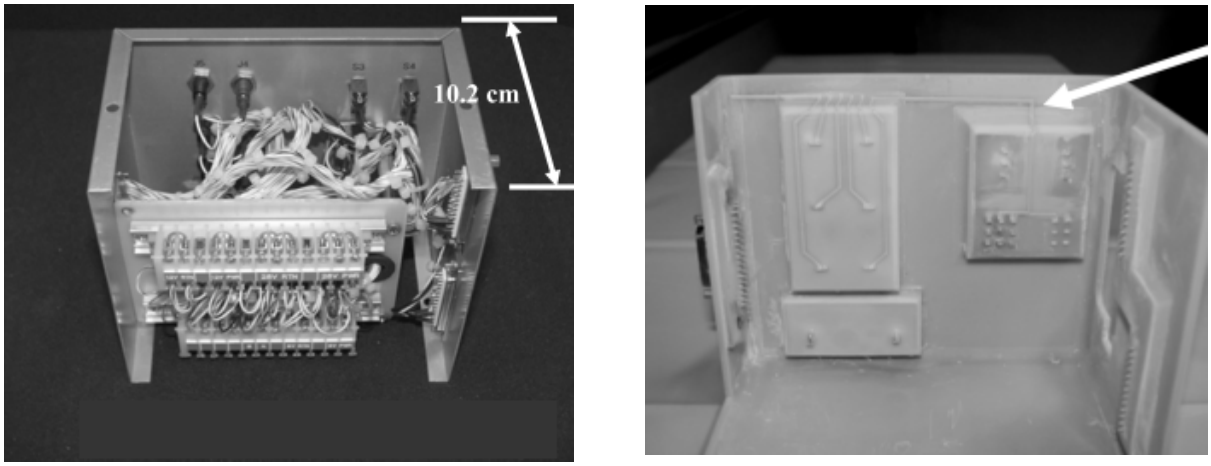

Figure 2.4 : Comparison of traditionally assembled electrical junction box and (b) junction box manufactured using direct write and additive manufacturing used under fair use, 2013 [1]

In 2006, Robinson and coauthors created embedded interconnects using ultrasonic consolidation (UC) and pneumatic extrusion-based direct write to fabricate signal routing in a cellular aluminum panel [29]. The electronics are completely embedded in the robust and lightweight structure. Structural interconnects eliminate the need to design for cabling ducts and vias throughout a structure's interior. The circuit's encapsulation also protects interconnects from the outside environment. The substrate used was aluminum tape (Al 3003 H18). Artic Alumina thermal epoxy was used to secure the embedded components and to line the channels made for embedding electronics because of its electrically insulating qualities. E 1660 ink was used to create the directly written interconnects using a Nordson EFD 2405 Ultra Dispensing System, which is a pneumatic syringe-based system. Thermal curing was performed, although the specific times and temperatures are not specified. During the manufacturing process, the panel was removed from the UC build platform and moved to a 2-axis linear stage to dispense the desired geometry, as shown in Figure 2.6. After the deposition process, the UC process was resumed to fully encapsulate the conductors. The work reports a relative reduction in resistivity after encapsulation, although it is hypothesized to be due to the temperature of the ultrasonic consolidation process.

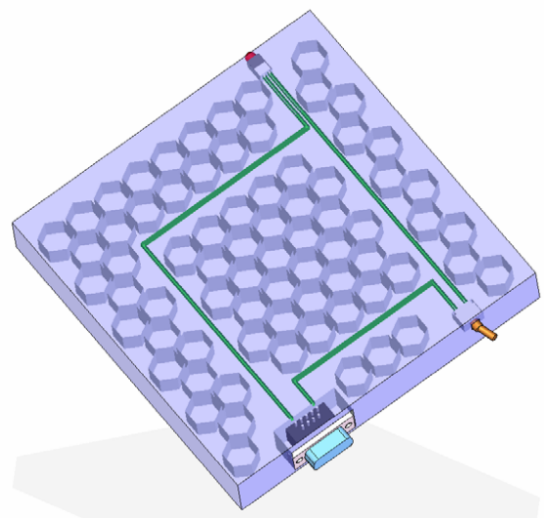

Figure 2.5: Cross sectional view of embedded circuit in honeycomb structure fabricated with the hybridization of UC and direct write used under fair use, 2013 [29]

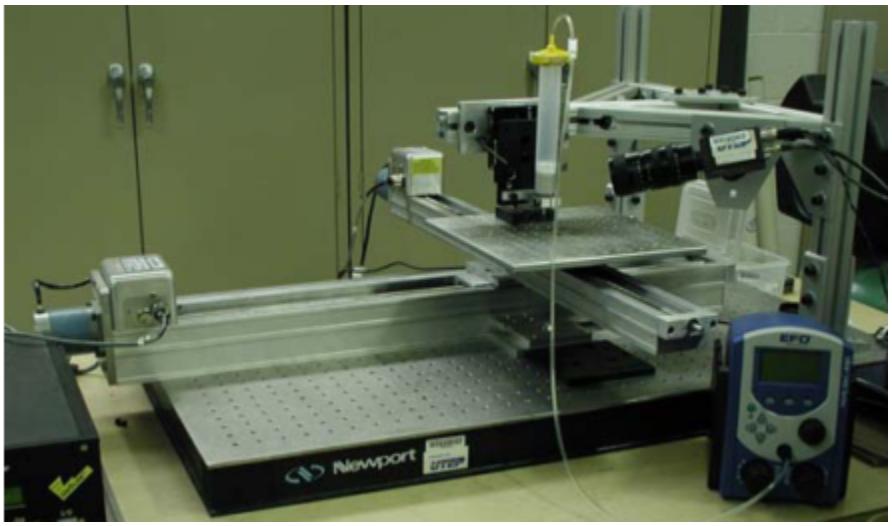

Figure 2.6: Direct write setup used under fair use, 2013 [21]

In 2013, Folgar and coauthors integrated both Aerosol Jet and Micropump technologies with laser sintering (LS) to fabricate conductive traces [3]. This study is unique in that it is the only work to utilize LS with direct write. Traces of Cabot CSD-32 and 40-3920 HVA silver-based inks were deposited by Aerosol Jet and Micropump technologies, respectively. The traces were deposited on prefabricated LS substrates (Figure 2.7) and heat treated according to supplier

recommendations (between 100°C and 300°C). While specific resistivity is not reported, continuity is confirmed in both processes.

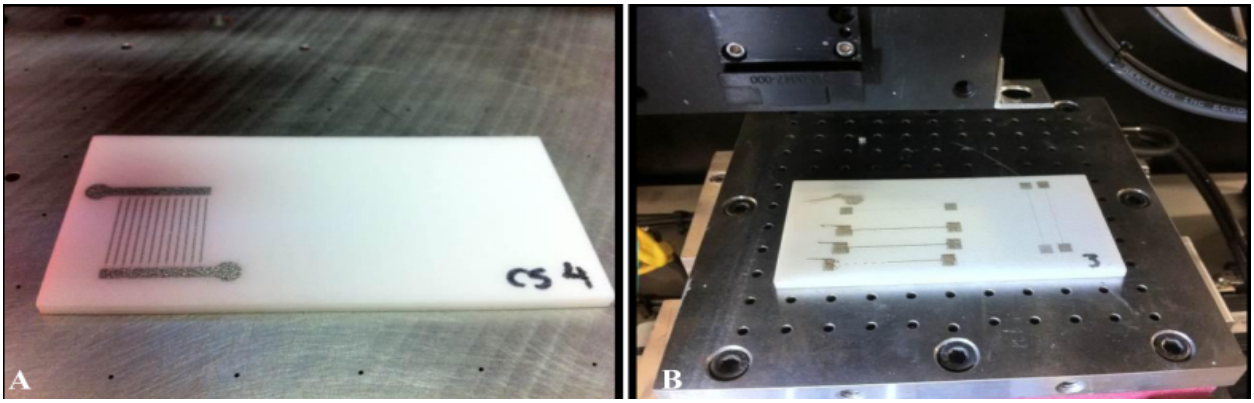

Figure 2.7: Traces of silver ink printed on SLS substrates using (a) Aerosol Jet and (b) Micropump dispensing used under fair use, 2013 [3]

One of few works to assess the feasibility of actually hybridizing direct write and additive manufacturing technologies, Folgar and coauthors retrofitted a Fab@Home mechanical extrusion-based direct write machine to deposit conductive materials. A Fab@Home machine was redesigned to fit into a DTM 2500CI SLS system as shown in Figure 2.8. The machine is capable of depositing traces in multiple layers; however, the authors cite the added difficulty of pausing the build at every layer to insert the machine, deposit material, and remove the machine if 3-dimensional interconnects are required. A machine that did not require removal for subsequent printing steps would alleviate this.

Figure 2.8: Redesigned Fab@Home mounted inside SLS machine used under fair use, 2013 [3]

2.3.2 Discreet Electronics

In 2005, Medina and coauthors used stereolithography and direct write to place a small camera and video transmitter within the internal structure of a printed alarm clock [21]. The camera embedded in the alarm clock showcases the ability to leverage AM's geometric reproduction abilities and the utility of conductive traces to create discreetly embedded electronics. The housing is created using Prototherm™ 12120 material because of its heat deflection temperature of 126°C for curing the metal loaded inks. CI 1002 silver ink from Engineered Conductive Materials was used to create the metal traces. The metal-loaded ink was dispensed on the finished SL part using a Nordson EFD 2405 Ultra Dispensing System, which is a pneumatic syringe-based system. The housing was fixed to a 2-axis linear stage to dispense the desired geometry as previously shown in Figure 2.9.

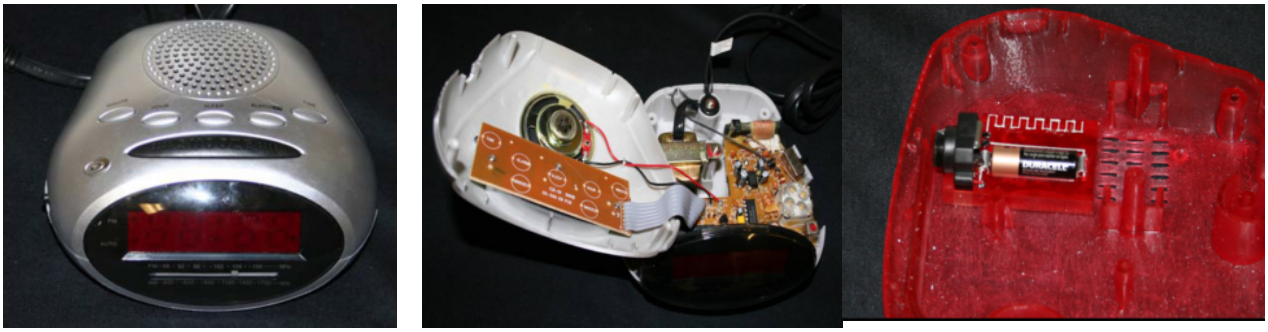

(a) **(b)** **(c)**

Figure 2.9 – (a) original alarm clock; (b) alarm clock internals; (c) printed base to incorporate wireless camera module used under fair use, 2013 [21]

2.3.3 Integrated Antennae

In 2013, Breyfogle and coauthors demonstrated the ability to use Aerosol Jet direct write to deposit conductive materials on fused filament fabrication (FFF) surfaces [27]. The work used ULTEM 9085 material, which has a heat deflection temperature of 153°C and is compatible with the curing conditions of metal loaded inks. The conductive materials were deposited to create a 1.3 GHz antenna shown in Figure 2.10. Printed parts were fixed on a 2-axis table and the Aerosol Jet process was used to deposit the conductive materials. A strain gage was attempted, but failed because of the surface quality of FFF components. This issue is discussed further in Section 2.4.2. Another issue encountered is that traces would fail because of cracking during

the curing process due to a mismatch in the coefficient of thermal expansion between the conductive material and FFF substrate. While not performed on an additively manufactured substrate, Breyfogle also demonstrated Aerosol Jet's ability to deposit on conformal surfaces demonstrating the technology's flexibility (shown in Figure 2.10).

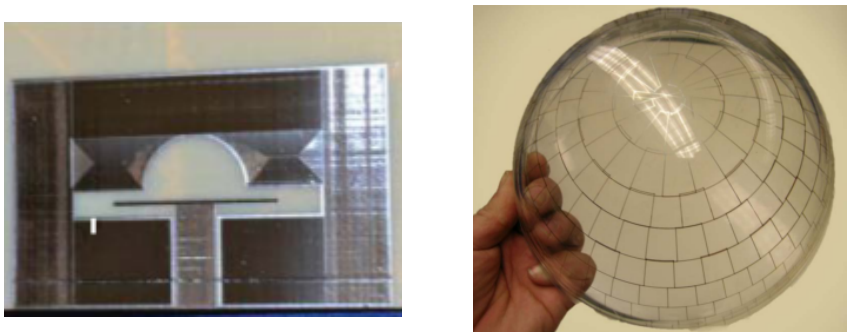

(a) **(b)**

Figure 2.10 – (a) 3-dimensional fractal antenna [30]**; (b) Aerosol Jet of conductive traces on conformal substrate; (c) Aerosol Jet of antenna on AM substrate used under fair use, 2013**[27]

2.3.4 Battery Fabrication

In 2008, Malone and coauthors developed and characterized a zinc-air battery created with a Fab@Home multi-material extrusion system [31]. The zinc-air battery is capable of an energy density up to 1.07 mW/cm^2. This work is unique in that it uses mechanical screw extrusion for both the conductive and structural materials. The work utilized silicone for the enclosure, silver-filled silicone as a conductor. The silicone conductor is chosen because it offers a similar bead size as the structural silicone and retains its as-deposited volume, whereas metal-loaded inks shrink as the solvent evaporates. The material is also used without a curing step. Specially designed zinc anode and cathode materials were also used to make the battery functional. With respect to feature size and conductivity, this example is not particularly extraordinary. It, however demonstrates the desirability of having a unified system capable of depositing both structural and conductive materials to seamlessly integrate multiple functional materials in a single part.

In 2013, Lewis and coauthors developed a lithium-ion battery design using extrusion processing with a power density of 2.7 mW/cm^2 [32]. The lithium battery is very small (6.6 mm^3)

and comprised of specially formulated anode and cathode materials. A novel curing process for preserving structural integrity is used and discussed in Section 2.4.3. The process relies on a separate substrate with a gold on glass current collector and packaging. While only requiring direct write technology, it is feasible that such an assembly could be embedded in an additively manufactured component.

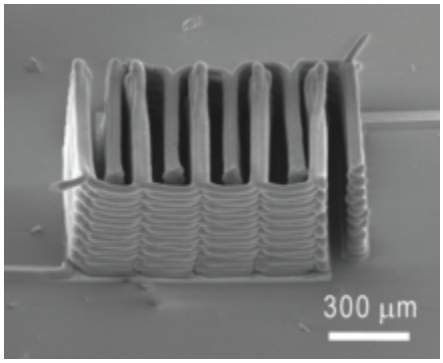

Figure 2.11 – SEM images of additively manufactured battery electrode used under fair use, 2013 [32]

2.3.5 Conformal Electronics

Conventional fabrication of high density circuitry relies on flat substrates because of process steps such as lithography which require a planar surface. However, products that benefit from complex geometries, such as wearable technology, rely on conformal geometries to better fit the user. Castillo and coauthors applied conductive materials to conformal substrates fabricated using stereolithography to showcase wearable technology [33]. A skull-conforming helmet insert was fabricated using ProtoTherm™ 12120 resin and E1660 silver-loaded conductive ink. The ink was used for electronic interconnects and to fabricate an antenna. Because of the conformal geometry, an automated direct write process is not used. Rather, the conductive ink was applied manually using a syringe. No information is given in the published literature regarding ink curing conditions. Figure 2.12 shows the helmet fabricated using stereolithography, IC components, and manually deposited traces of silver ink [34].

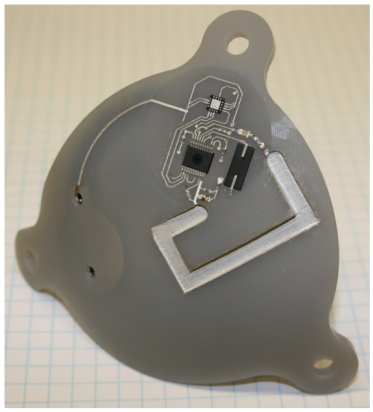

Figure 2.12 – Helmet insert for detecting traumatic head injury used under fair use, 2013 [33]

2.4 Potential Roadblocks and Challenges of Integrating Direct Write and Additive Manufacturing

The hybridization of direct write and additive manufacturing is non-trivial because of (i) material post-processing temperature compatibilities, (ii) adhesion between conductive and substrate, and (iii) adhesion between conductive layers. The following subsections discuss these issues in detail and provide potential solutions when possible.

2.4.1 Temperature Processing

Most of the work done in the past decade in combining AM and direct write has been confined to selecting AM materials that can withstand high temperatures and direct write materials that require relatively low post-processing temperatures. For example, most metal direct write inks require post processing at a minimum of 100°C to become conductive. Only a few polymeric AM materials can withstand these temperatures. Some of these materials include Duraform HST™ (powder bed fusion), ProtoTherm™ (vat photopolymerization), and ULTEM™ (material extrusion). In contrast, the most temperature resilient PolyJet material (RGD 535) has a glass transition temperature of only 65°C [35].

High temperatures allow individual metal particles to form necks and eventually grain boundaries. This neck and subsequent grain boundary formation increases contact area and, consequently, conductivity. The temperature at which diffusion and sintering occur is different

for different metals. This is typically at least 70% of the material's melting temperature, which is near 700°C for metals. The melting temperatures of metals in particle decreases when the particles are sufficiently small [36]. Figure 2.13 demonstrates how melting temperature decreases as particle diameter also decreases. One conclusion is that sufficiently small particles on the nanoscale could sinter at low temperatures compatible with AM substrates.

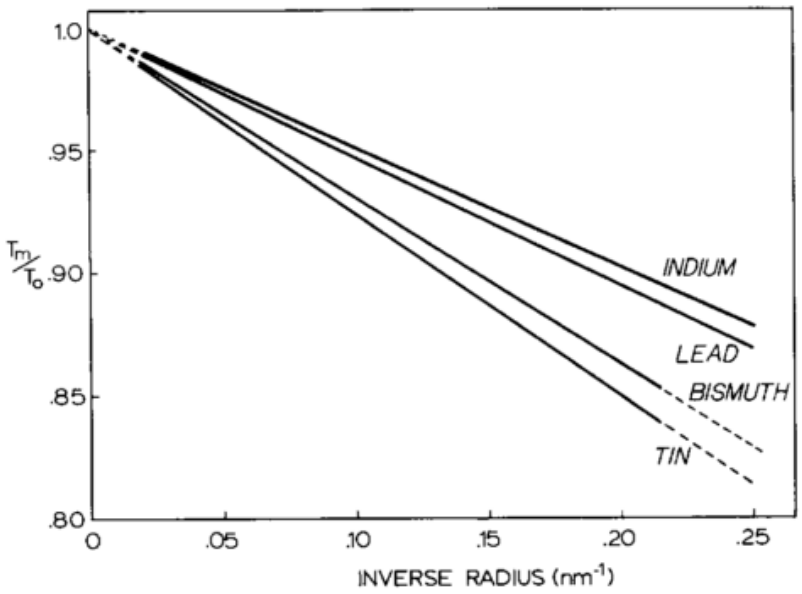

Figure 2.13 – Melting temperatures as a function of particle radius demonstrating lowered melting temperatures as size decreases used under fair use, 2013[36]

As the diameters decrease into the nanoscale, inter-particle forces begin to dominate the suspension of the particle-solvent mixture. Maintaining a homogenously dispersed mixture becomes a challenge. Resulting agglomerates of the particles are larger than their singular, dispersible, counterparts. Agglomerates are difficult to dispense without clogging. It is possible to coat the metal particles with capping agents to prevent agglomeration; however, the capping agents themselves require high temperature processing for removal. The capping agents then become the limiting factor for post-processing temperature.

Figure 2.14a shows particles still encapsulated by the capping agent, which prevents agglomerations while in solution form. At this stage, the material is only slightly conductive, if at

all. Figure 2.14b exhibits the interfacing of the particles after the capping agent is removed. Temperatures of at least 100°C are typically required for this. Figure 2.14c demonstrates low temperature sintering. Based on Ostwald ripening, surface particles have migrated to more stable sites, lowering the overall surface energy [37]. This results in densification and more contact area between particles. However, at its limit, the resulting structure is still porous and, thus, not as conductive as the bulk material. Figure 2.14d shows a fully sintered and dense formation. This formation reaches the conductivity of the bulk metal, but it requires temperatures of 70-90% of the materials melting temperature. Perelaer and coauthors provide a more extensive review of conductive inks and the factors governing their post-process requirements [38].

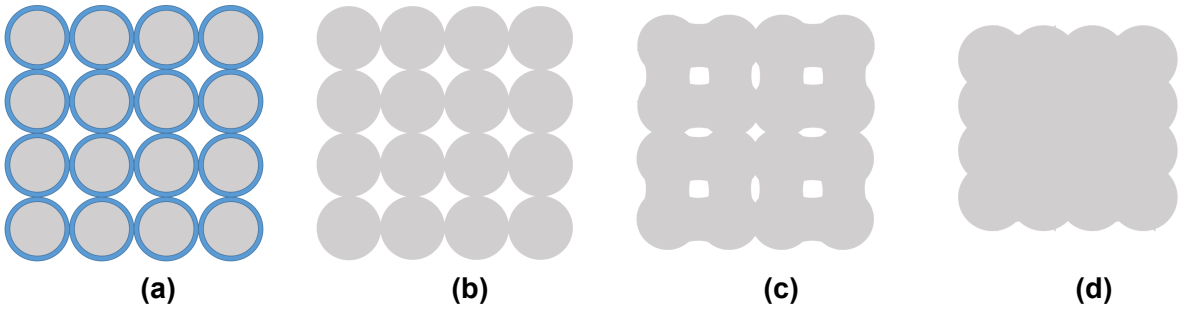

Figure 2.14 – Different stages of post-processing to improve conductivity of particle-based metal inks

Achieving high conductivity DW traces in AM requires a substrate material capable of surviving sintering temperatures. For example, Medina, Wicker, and Lopes combined Stereolithography and Micropump direct write technologies to create electrical interconnects printed onto additively manufactured structures with Heraeus PC 5915 silver-loaded ink. This is accomplished by taking advantage of high-temperature resins (DSM Somos ProtoTool™) that can withstand the 110°C post-processing temperatures required by their inks [9], [13], [29], [33], [34], [39].

When integrating direct write with the PolyJet process, it is not likely that sintering of the deposited inks will be possible due to temperature incompatibility. Therefore, the conductivity will be largely a function of particle to particle contact as shown in Figure 2.14b. Hence, metal inks with high metal loadings are desired because of their high particle density.

2.4.2 Interaction between Direct Write and Additive Manufacturing Materials

For any deposition process, adhesion between the deposited material and substrate is important. Poor adhesion between the materials can result in delamination of the conductive materials from the substrate and failure. This is especially important for traces that are embedded within a print and not on the surface. After a circuit is embedded, access and repair is not possible. It is difficult to discern without testing if the adhesion between particular inks and AM substrates is possible. Factors influencing adhesion include:

- Surface energy of both direct write material and AM substrate
- AM substrate surface roughness
- AM substrate surface treatment
- Chemical interaction between direct write and AM materials

The surface energy of the direct write material and AM substrate can determine the contact angle between the materials or surface wetting. Better wetting implies more contact area, more surface energy, and thus better adhesion [40]. The surface roughness of the AM substrate also can affect the adhesions characteristics. Cheng and coauthors [41] determined that the surface roughness could be especially important to the adhesion of microparticles on a substrate. A surface with largely varying surface roughness on the microscale was shown to reduce pull off forces and thus be less adhesive. Smoother surfaces are shown to promote adhesion on the microscale. At a macroscopic level (hundreds of microns and larger), surface roughness provides more contact area and actually promotes adhesion. A more detailed explanation of these interaction can be found in [41]. Surface treatments such as etching, plasma treatment, and priming can change the surface tension of substrates to enhance adhesion characteristics [42], [43]. Finally, a chemical interaction between the direct write material and AM substrate can also contribute to the adhesions characteristics of the parts. Understanding these parameters is important to achieving good adhesion.

Additive manufacturing technologies pose unique challenges with respect to surface adhesion because of the surfaces that they produce. For example, fused filament fabrication

(FFF) has a very non-uniform surface on the macro scale, which poses a unique problem for direct write. FFF produces a ridged surface because its material patterning process.

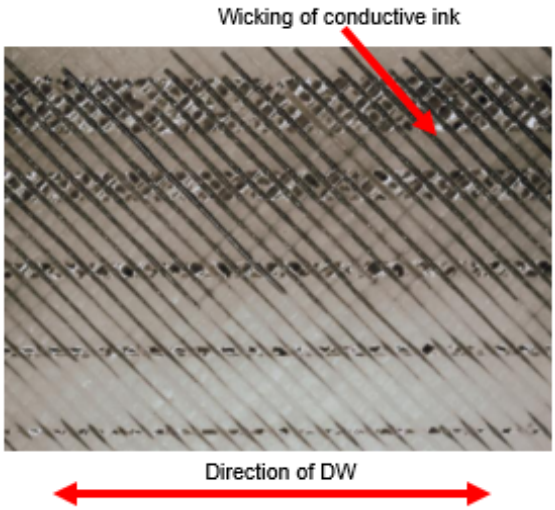

Figure 2.15 – Close up image of silver inks deposited on FFF ULETM 9085 printed substrate used under fair use, 2013 [44]

Figure 2.15 is a magnified image of silver ink deposited on an FFF surface. Since the surface is not flat, conductive inks tend to fill into the valleys between the AM traces resulting in short circuits or discontinuities. Optomec and Stratasys utilized an ultra-violet (UV) curable dielectric material as an intermediate bonding layer between the FFF part surface and the conductive ink [44]. The dielectric material fills the voids and dries with a planar surface as shown in Figure 2.16 .

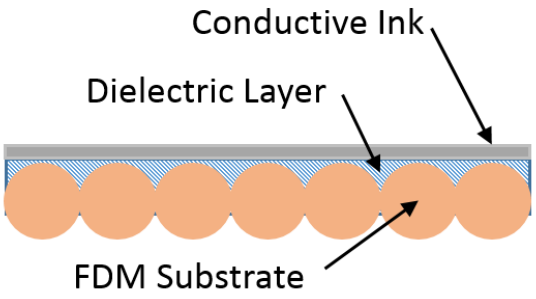

Figure 2.16 – Conductive ink deposited on FFF substrate using dielectric intermediate bonding layer

The dielectric material creates a flat surface for depositing conductive material. The dielectric can also be chosen with good adhesion characteristics to both the substrate and conductive materials. For this reason, an intermediate layer could also be used with other AM processes such as stereolithography to benefit adhesion, even if the surface is much smoother than that of the FFF process. Because of the flexibility of direct write systems, it is possible to use the same systems for depositing the dielectric material.

Moreover, an intermediate bonding layer can help to alleviate stresses induced by a mismatch in the CTEs of the AM and conductive materials, which is common between a metal and a plastic. Sintering elevates the temperature of the conductive material and cracking may occur if the difference in CTEs is sufficiently high, as discussed in Section 2.3.3.

2.4.3 Interlayer bonding and conductivity

Interlayer bonding is an important aspect of DW to consider in the context of AM because a multilayered process is inherently more compatible with AM process. Moreover, it enables more complex circuit geometries and configurations within a part. Previous research regarding DW of circuits has largely focused on planar, single layer, deposition because of its applications in PCB fabrication. Many of the hybridizations of DW and AM so far have only incorporated these single layer DW methods. While DW has been shown feasible on 3-dimensional conformal surfaces, the deposition is still done in a single layer [34].

Lopes and coauthors have shown DW compatibility in three-dimensions with deposited vias [9]. This process combines stereolithography (SL) and extrusion-based DW. Figure 2.17 diagrams the process. First, IC components are embedded in a partially completed build. A second build process creates vertical interconnects for connecting the embedded components. The stereolithography build finishes with traces to connect all the embedded components. The extrusion-based DW process finally dispenses conductive ink in the traces and into the vias. The vertical interconnects are explicitly cited as a potential manufacturing and design issue. They require direct access from the surface and complex channels can be difficult to fill with ink. In situ multilayer deposition would allow for conductive materials to be deposited layer by layer in conjunction with the corresponding AM process and alleviate the design complications of the vias with designs that do not require access from the surface. However, bonding between the layers of conductive inks is a critical issue.

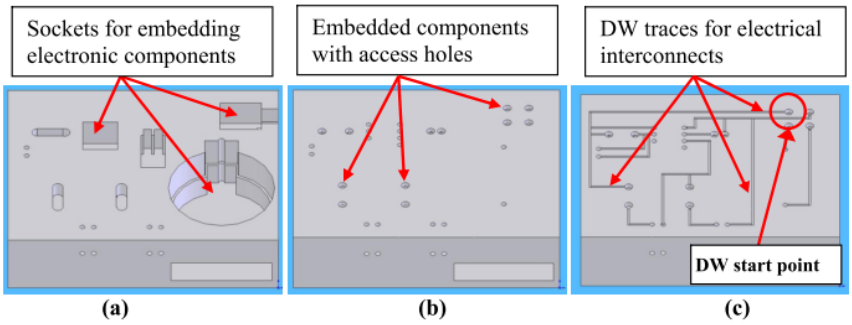

Figure 2.17 – Build stages for DW and SL incorporating vertical interconnects. (a) sockets for embedded components; (b) vias to access embedded components (c) planar interconnects used under fair use, 2013 [9]

Multilayer DW is desired in the hybridization of DW and AM to leverage the full capabilities of the AM process. Layered DW allows for multiple layers of circuitry in a single build as well as conductive features orthogonal to the build plane. However, it has been shown that in layer-based deposition of conductive materials, the conductivity along the plane of depositions is higher than conductivity between layers, perpendicular to the plane of deposition. [15]. This is due to lower contact density between layers versus along layers. Good interlayer bonding minimizes this.

A potential solution to promoting interlayer bonding and, hence, conductivity is a graded volatility solvent. Sun and coauthors have shown this type of solvent to promote adhesion between layers so that printed structures can withstand sintering without delamination and distortion [32]. Water is used to enable the deposited layer to dry enough to solidify and maintain shape. Ethylene glycol and glycerol are also part of the solvent to maintain moisture after the water has evaporated to promote interlayer bonding. Once the structure is finished, the other solvent constituents can be removed with temperature processing. This is one potential solution to creating solvent-based inks that are compatible with AM processes yet maintain conductivity.

2.5 Conclusions Based on Previous Works Combining Direct Write and Additive Manufacturing Technologies

Having reviewed the strengths and limitations of different direct write materials and technologies as well as previous attempts to combine additive manufacturing with direct write, this section summarizes the major considerations of combining the two technologies.

Carbon-based inks are the least conductive and not ideal for electronics applications beyond electromagnetic shielding and electrostatic dissipation. However, they are much less expensive than their metal-based alternatives. Metal-based inks are much more conductive (2-4 orders of magnitude) than carbon inks. When sintered, both metal-loaded and MOD inks approach the conductivity of bulk metals. MOD inks are advantageous in that their rheology may be tailored to the needs of the dispensing technology. However, their metal content by weight percent is limited. Metal-loaded inks may have upwards of 70% metal by weight. Therefore, as-deposited and without sintering, metal-loaded inks may provide a denser and, thus, more conductive product. In reviewing direct write technologies, material choice hardly restricts process selection because each process is capable of depositing a formulation of the different ink types.

Of the direct write technologies reviewed, Aerosol Jet is the most flexible but also the most expensive. Aerosol Jet can dispense any ink that can be aerosolized and the toolhead offset from the substrate is less critical than with other technologies. The throughput of Aerosol Jet technology, however, is very low. Serializing toolheads is possible but increases cost. The unsintered conductor density is unclear but likely less than with extruded metal inks. Published works have only analyzed sintered conductor density.

Inkjet technology is limited in its material compatibility due to nozzle clogging issues and the required rheology for droplet formation. Moreover, the toolhead offset from the substrate is critical, making the process more complex. Single inkjet orifice throughout is very low, although inkjet print heads are commonly serializes to compensate. Because of the limitations on metal loading, as-deposited unsintered conductors will also have a low material density and thus lower conductivity.

Extrusion direct write systems provide the most flexibility in terms of material capabilities. Heavily loaded inks can be dispensed with extrusion system, although feature resolution may be

negatively impacted. The tolerance in toolhead offset from the substrate surface is less flexible than Aerosol Jet, but more so than inkjet. The throughput of extrusion based systems is relatively high. Because extrusion based technologies can dispense heavily loaded inks, the deposited conductor density before sintering is likely to be higher than with any of the other technologies.

Previous works have used metal-based inks exclusively. This is attributed to their availability and conductivity. Extrusion technologies are popular because of their ability to dispense viscous materials and their low cost. Common challenges include temperature processing, material adhesion, and interlayer bonding, although these are not specific to extrusion-based DW. Most examples have used additive manufacturing materials that can withstand the curing temperatures recommended for metal-loaded inks. DW technology selection will need to account for which system can deposit the densest conductor without sintering because of PolyJet materials' temperature incompatibility. Few of the previous works have investigated the adhesion characteristics between the conductive material and substrate. Breyfogle and coauthors warn that non-uniform surfaces may be problematic because of CTE mismatches. Folgar and coauthors explain the difficulty of multilayered conductors because of interlayer conductivity and the time required to switch between processes at every layer. Using these lessons from previous works, Chapter 3 describes the process and rationale in designing the direct write system for hybridization with the PolyJet process.

3 DESIGN OF A DIRECT WRITE SYSTEM FOR INTEGRATION WITH THE POLYJET PROCESS

The primary goal of this work is to create embedded electronics by combining direct write and PolyJet technologies. The design of the direct write system for this purpose is detailed in this section. Before understanding how conductive materials may behave on a PolyJet substrate, a reliable mechanism for depositing conductive materials must be designed and embodied. This chapter synthesizes the customer needs of the project into tangible engineering metrics to guide the machine's design.

3.1 Mission Statement

The mission statement is presented as the first step in the machine design. It serves to unify information about the objectives of a project, limitations, and projects stakeholders. The mission statement also identifies potential avenues for creative design in the project where truly innovative solutions may be applied. Ultimately, the mission statement serves as a reference point later in the design process to ensure that the original goals are being met in the eyes of the stakeholder.

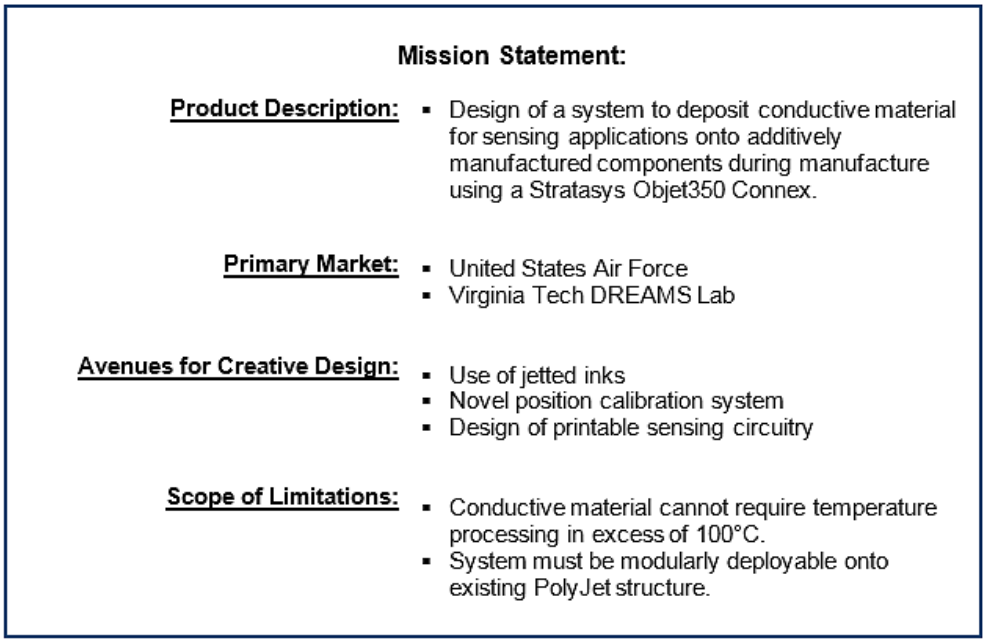

Figure 3.1 Mission Statement

3.2 Quality Function Deployment (QFD)

Using the operational understanding gained from the literature review (Chapter 2) and mission statement, system functions and capabilities are refined as customer needs. This section explicitly explains the major customer needs and uses Quality Function Deployment (QFD) to define engineering metrics that can be used to benchmark how well the system meets those customer needs. Moreover, QFD analyzes the interdependencies between the customer needs and engineering metrics. This way, customer needs that influence multiple engineering metrics can be deemed more important than those only affecting few or one. This importance ranking combined with weighted importance of the customer needs is used to rank the importance of the overall customer needs. It is important to note that while the machine is to be designed for depositing conductive materials, the literature review demonstrates that the conductivity is primarily a function of the materials used and not the direct write technology selected. Electrical performance (conductivity) can thus be considered independently of deposition mechanism. The customer needs are defined in the following subsection beginning with the most important.

3.2.1 Customer Needs

The system cannot interfere with the PolyJet Process

Because this system is designed to operate in conjunction with the Objet process, the deposition system cannot interfere with its operation. From the functional model, the system must be able to deposit conductive material while a PolyJet print is paused and the PolyJet system must also be able to resume printing post-deposition.

System should fit in the PolyJet machine

It is possible to remove a printed part for processing during a print and then replaced after processing to resume printing. However, because of the PolyJet's high-resolution capabilities, accurate replacement of an unfinished part would require repeatable placement accuracy of less than 32 microns. Because of this implied constraint, it was decided that the deposition system be placed into the PolyJet machine for processing directly on the printed substrate on

the build tray. As a result, the need for the machine to fit in the PolyJet machine is a requirement.

Deployment and removal should be easy

Having decided that the system should fit in the PolyJet machine, a secondary customer need arises, which is that the machine should be easily deployed and removed. In the next section, the metrics that qualify easy operation are discussed.

Deposited features should be compatible with the PolyJet's resolution capabilities

The PolyJet process is capable of a resolution of 42 micron in the X- and Y-directions and 32 microns in the Z-direction. The selected deposition system should have relatively similar resolution capabilities.

Operation should be simple

As with any developed processes, simple operation is desired. Fewer processing steps and less user intervention is ideal.

A high level of automation is desired

This customer need requires that when possible, processes be automated. While this is not such a strict requirement during the prototyping phase, the final design should incorporate automation whenever possible.

The deposition process should be possible in a reasonable amount of time

Different direct write technologies have different deposition speed capabilities. The design should select a technology that can deposit material efficiently and quickly relative to the PolyJet's material deposition speed. While the speeds may not match exactly, the direct write process should not dramatically increase the total production time.

3.2.2 Engineering Metrics

Engineering metrics are a set of metrics derived from the customer needs. The main distinction from customer needs is that engineering metrics have a direct way of being measured. One or more metrics are brainstormed for each customer need.

Difference in print heights (minimize) [μm]

For most additive manufacturing technologies, the layer thickness or print height is a governing factor for resolution in the Z-direction. For the PolyJet process, the layer thickness is 32 μm. It is useful to selection a deposition method that is capable of matching this layer thickness closely. Matching this thickness helps to ensure process compatibility. Smaller layer thickness would require multiple layer of deposition and lead to longer printing times. Larger print heights would not be able to leverage the high resolution capabilities of the PolyJet process.

Number of steps (minimize)

The number of steps required to operate the machine from insertion to removal is measured to indirectly gage the difficulty of the direct write process. Fewer steps is an indicator of simplicity.

Gross Volume (minimize) [m^3]

Because of the easy to deploy and remove requirement and the need to fit into the PolyJet printer, gross volume is an important metric. Minimizing volume leads will allow it to be easily moved and fit onto the PolyJet build platform.

Net Weight (minimize) [kg]

Again, because of the easy-to-deploy and remove need, reduced weight is a key metric. A lighter design makes the machine easier to manually move. This metric also helps to ensure that the machine is not too heavy for the PolyJet machine itself to support.

Minimum feature size (target) [μm]

Minimum feature size of depositions is also important to matching the capabilities of the PolyJet process. Much like the minimum print height, larger feature sizes do not leverage the high resolution capabilities of the PolyJet process. Features that are too small would dramatically increase processing time.

Linear deposition rate (maximize) [mm/min]

Linear deposition rate is important to the speed of the process. Slow deposition is undesirable because it increases processing time.

3.2.3 Discussion of the House of Quality

Every element in the central matrix of the House of Quality (Figure 3.2) represents the strength of the relationship between the corresponding customer need and engineering metric. The triangle, hollow circle, and solid circle represent weak, moderate, and strong relationships, respectively. Following the columns of the central matrix, it is shown how many different customer needs a single engineering metric may affect.

By aggregating these relationships in the form of a technical importance score, metrics that have a more influence on meeting customer needs are deemed more important by their relative weight. Technical importance is calculated by the summation of the strength of the relationship between the customer need and engineering metric multiplied by the ranked customer importance as shown in Equation 3.1. Relationships (j_r) that are weak score 1, moderate score 3, and strong relationships score 9. The customer importance (k_i) is ranked from 5 to 10 with 10 being the most important.

$$\textbf{Technical Importance} = \sum \mathbf{j_r k_i} \qquad \text{Equation 3.1}$$

According to the House of Quality, the three most important engineering metrics are (i) volume, (ii) feature size, and (iii) print height. Volume impacts four different customer needs with two strong and two moderate relationships. Therefore, the system's overall volume is paramount. Beyond a certain size, the machine would not even fit on the PolyJet platform, which is a must. Deposited feature size is also very important. Poor resolution would not leverage the capabilities of PolyJet. A target is set at 65 μm, which is twice the droplet resolution of the PolyJet process. While better resolution from a direct write process is possible, a

particular technology would not necessarily be considered better for having a smaller resolution beyond the target. Print height is just as important as the feature size metric. It relates to the PolyJet resolution in the same way, although in the vertical direction. This metric is a target set at 32 μm, which is the layer height of the PolyJet process. These metrics and their relative importance will guide the embodiment design of the direct write process.

QFD: House of Quality

Project: Conductive metal deposition mechanism

Revision: 1

Date: 9/12/12

Row #	Weight Chart	Relative Weight	Customer Importance	Maximum Relationship	Customer Requirements (Explicit and Implicit) \ Functional Requirements	Δ Print Heights (µm)	Number of Steps	Gross Volume (m^3)	Net Weight (kg)	Minimum Feature Size (µm)	Linear Depostion Rate (mm/s)
					Column #	1	2	3	4	5	6
					Direction of Improvement	◇	▼	▼	▼	◇	▲
1	|||||||	20%	10	9	Doesn't interfere with PolyJet process	●		○		●	
2	||||||	12%	6	9	Easy to operate		●	○	○		
3	|||||||	18%	9	9	Fits in PolyJet machine			●	▽		
4	|||||||	16%	8	9	Easy deployment & removal		○	●	●		
6	|||||||	14%	7	9	Matches PolyJet feature size capability	●				●	▽
7	||||	8%	4	9	Deposits in a timely manner	▽	▽			○	●
8	|||||	10%	5	9	Highly automated		●				▽
					Target	32	0	0	0	42	Infinity
					Max Relationship	9	9	9	9	9	9
					Technical Importance Rating	320.4	259.2	410.2	202	336.7	97.96
					Relative Weight	20%	16%	25%	12%	21%	6%
					Weight Chart	||||||| ||||||| ||||||| |||||| |||||||	

Correlations	
Positive	+
Negative	−
No Correlation	

Relationships	
Strong	●
Moderate	○
Weak	▽

Direction of Improvement	
Maximize	▲
Target	◇
Minimize	▼

Figure 3.2: House of Quality

3.3 Component Selection

3.3.1 Dispensing Mechanism

For material dispensing, extrusion-based direct write is selected because of its ability to dispense viscous metal loaded inks with high loadings. Because sintering is not possible due to the PolyJet substrate's temperature incompatibility, heavily loaded inks are desired to deposit a dense conductor. A Nordson EFD Ultimus V high precision dispenser is used for this purpose. The dispenser uses air pressure to dispense materials via a syringe. The Ultimus V can be used to deposit a range of material with ranging viscosities and material loadings including the DuPont 5021 ink. Positive pressure from 0-100 psi in increments of 0.1 psi can be applied to the syringe to extrude material, and a vacuum can be applied quickly to stop the material flow. Additionally, it has the ability to consistently meter materials from the syringe as the material level changes (nearly full versus nearly empty syringe). This removes the material metering control loop out of the larger control system, thus allowing for repeatable deposition control. While the literature suggests achievable resolutions of 25 μm by extrusion based systems, the resolution capabilities of the DuPont material from this specific dispenser will need to be characterized (Section 4.1).

3.3.2 Conductive Material

DuPont 5021 conductive material was chosen as the conductive direct write material because of its high conductivity, high flexibility, and ability to dry at room temperature [46]. From the literature review, it is concluded that metal loaded inks provide the highest conductivity without sintering because high metal loadings imply better conductivity. DuPont 5021 has a 70% silver loading by weight. Moreover its flexibility is desirable because of the need to deposit on flexible PolyJet substrates. Other, less heavily loaded variations were used including DuPont 5029 and 4817N. The 4817N is a low viscosity variation formulated for spray deposition. This low viscosity mixture had a large slump on the PolyJet substrate and resulted in a sparse and discontinuous distribution of metal particles on the substrate after the solvent evaporated. The 5029 is similar to the 5021, but with a lower solids loading (50% opposed to 70%). While this material was depositable, it also had a larger slump which negatively affected resolution. For these reasons, DuPont 5021 was chosen.

3.3.3 X-Y Motion Frame Design

The X-Y linear motion frame is designed from extruded aluminum framing because the material is lightweight, readily available, and has modular mounting options. The frame creates a sturdy base custom-sized to fit on the Objet 350 Connex build tray. The Y-stage uses two lead screws driven by synchronous stepper motors. The X-stage similarly uses a lead screw driven by a stepper motor. A one-inch lead screw pitch and 200 pole stepper motors result in a minimum system resolution of 125 μm per step. The pillow blocks, motor mounts, and toolhead holder were design to be printed by the Connex 350. This allowed for rapid manufacture of space-saving mounting components and easy shaft alignment when mounted to the extruded aluminum framing.

The motors are driven by Geckodrive 210X stepper motor drivers. An Arduino running grbl firmware (an open source g-code interpreter) interprets standard g-code into step signals for the motors. G-code is an industry standard for computer numerical control and is supported by multiple platforms which enhances the automation capabilities of the machine.

3.4 Machine Embodiment

Using customer needs as benchmarked by the engineering metrics, a machine was designed for depositing conductive materials during the PolyJet printing process. The direct write setup is presented below in Figure 3.3. After the PolyJet process has been paused at the appropriate layer, the machine is placed on the PolyJet build tray to deposit conductive material. The X-Y frame is made from extruded aluminum framing to fit on the Connex 350 build tray. Stepper motors are used to drive lead screws for X- and Y-direction translation and are controlled by an Arduino programmed to interpret basic g-code. DuPont 5021 silver loaded conductive ink is dispensed from a Nordson EFD Ultimus V air powered precision fluid dispenser. Dispense commands are also driven by the Arduino and interpreted from the g-code. The rationale for selecting the components as they relate to the engineering metrics is discussed for each main subsystem in the following subsections.

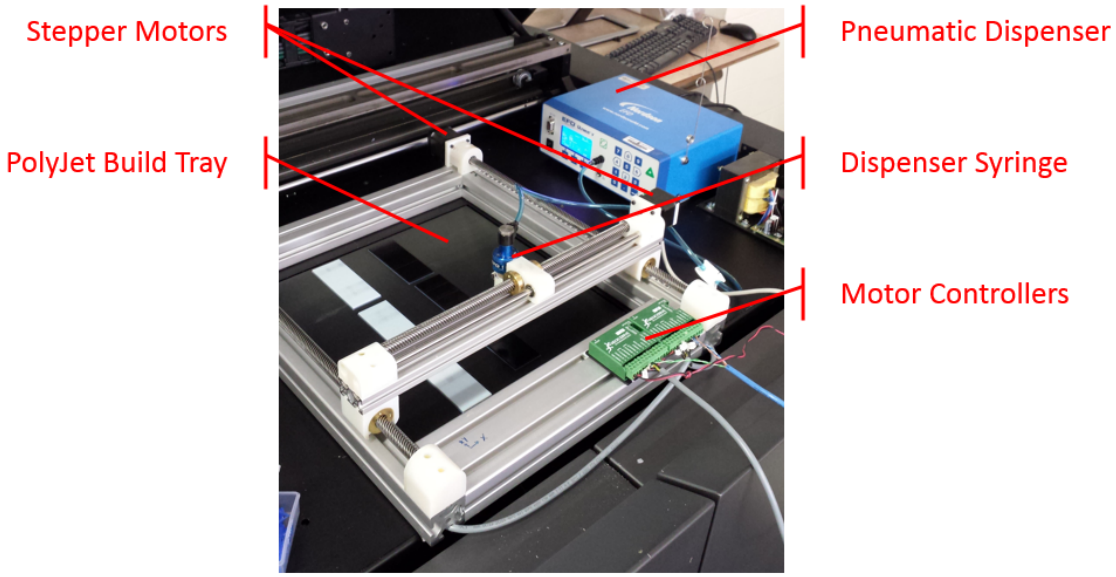

Figure 3.3: Direct write setup for PolyJet Process

3.5 Image-based build tray orientation and platform

An obstacle facing the implementation of a hybrid direct write system is that the deposition motion system and PolyJet build tray do not share common work coordinates. This is a problem with many hybridized industrial systems. The proposed solution to this is to utilize image feedback to detect the offsets between the two machines and compensate by altering the tool path of the direct write system. The general process is illustrated in Figure 3.4.

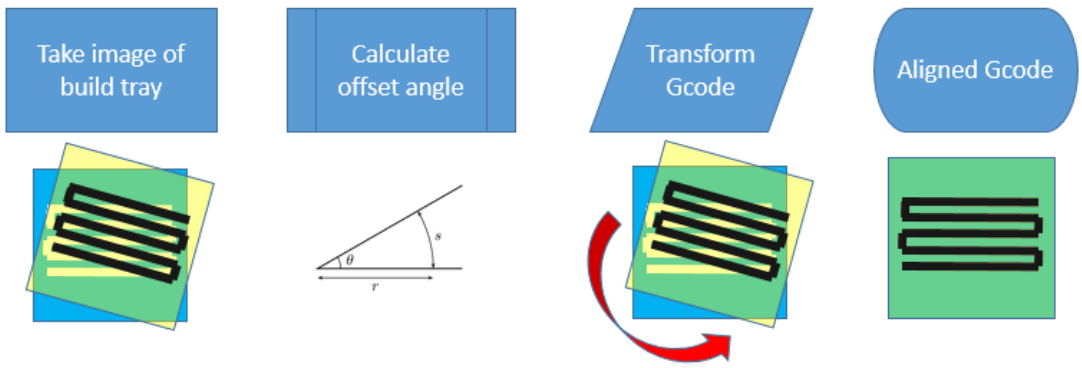

Figure 3.4: Process flow for compensating for machine misalignment

LabVIEW's vision and motion toolbox is well suited to detect the offset between the two machines. First, it is important that both systems have optical identifiers for alignment. The deposition mechanism has been marked with two dark lines that identify the X- and Y-axis. For the PolyJet system, two lines of the VeroWhite+ material are printed during the build for alignment. These markers are used to calculate the offset angle later in the process. The markers on the deposition system are shown in Figure 3.5.

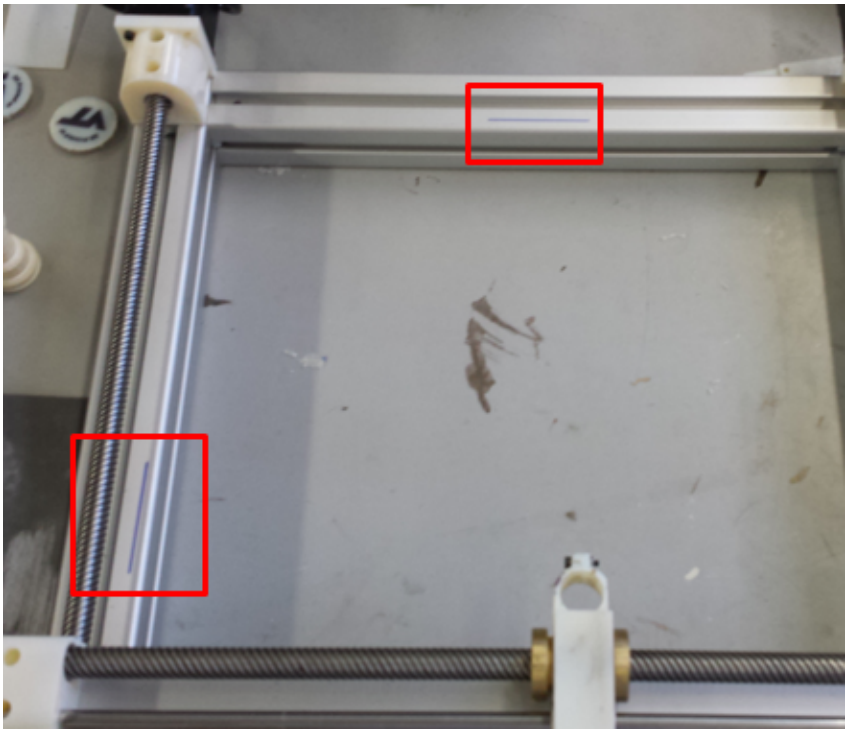

Figure 3.5: Optical alignment markers on direct write system

Once the deposition system is placed on the PolyJet's build tray, a camera is used take an image from above. The image photographs the build platform. LabVIEW's edge detection algorithm is used to locate any of the optical alignment indicators on the build tray and direct write system. When at least one line from each system is detected, LabVIEW can calculate the offset angle between the two systems. While the field of view is limited, Figure 3.6 shows lines detected in LabVIEW and in this example, a 3 degree deviation of the two coordinate systems is calculated. Using Equation 3.2, this rotational transformation can be applied to the X and Y coordinates of the toolpath's g-code so that it is aligned with the PolyJet's coordinate system. Future work will analyze the amount of misalignment that the system can compensate.

$$x' = x\cos\theta - y\sin\theta$$
$$y' = x\sin\theta + y\cos\theta$$

Equation 3.2

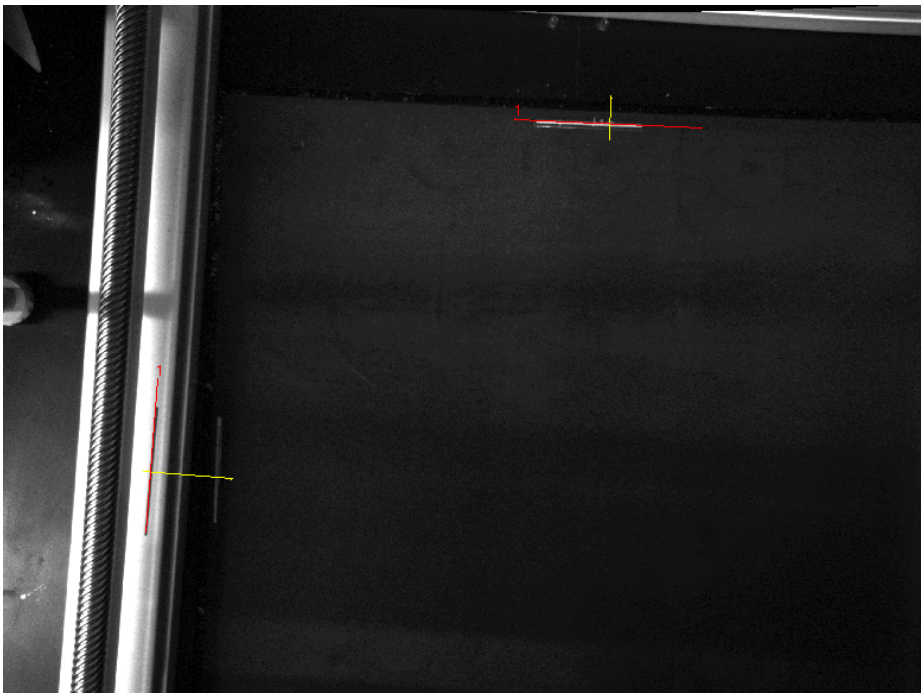

Figure 3.6: Sample image from LabVIEW showing detected lines from build tray image

With a system designed for repeatable deposition of conductive materials, it is possible to explore (i) the resolution limits of the deposition system, (ii) the interaction between the ink and substrate using PolyJet material compatible drying conditions, and (iii) the ability to embed and encapsulate the deposited conductors using the PolyJet process.

4 RESULTS AND ANALYSIS OF DIRECTLY WRITTEN CONDUCTIVE INKS ON POLYJET SUBSTRATES

To better understand how the deposition machine and conductive materials perform, four main research questions (RQ) are investigated in this section:

- **RQ1:** How do tip size, dispense pressure, and tool head speed affect feature width?
- **RQ2:** How does drying time and temperature the geometry of the conductive inks on PolyJet substrates?
- **RQ3:** What are the adhesion characteristic between the conductive ink and PolyJet substrate?
- **RQ4:** How does embedding and encapsulation effect conductivity of directly written conductors?

In the following sub-sections, each research question is briefly explained, a hypothesis is developed, and experimental methods, results, and discussions are presented to aid in their investigation.

4.1 RQ1: How do tip size, dispense pressure, and tool head speed affect feature width?

In Section 3.2, it is explained that the customer needs of the system demand features sizes comparable to the PolyJet process and fast deposition rates are desirable. For the pneumatic extrusion-based dispenser selected, tip size, dispensing pressure, and tool head speeds are the main process parameters that influence the geometry of deposited beads of material [45]. While the review of direct write technology suggests that deposition resolutions from pneumatic solutions can match that of the PolyJet process (Section 2.2.1), this system still must be validated. Beyond the resolution qualification, this research question aims to assess how tip size, pressure, and speed affect deposition geometry, as measured by bead height and width on both VeroWhite+ and TangoBlack+ PolyJet substrates.

As the material passes through the tip orifice, the extrudate assumes the cross-sectional geometry of the opening. As the material reaches the substrate, it is expected to slump, creating a trace wider than the tip orifice. Nonetheless, smaller tip diameters will yield smaller features relative to features from larger tip sizes. However, there is a practical limit to the minimum tip

diameter used based on the material and clogging issues (Section 2.1). Because pressure is proportionally related to the volumetric flow rate, it is hypothesized that lower pressures will produce lower flow rates and thus smaller features, although insufficient pressure will not allow material extrusion.

Moreover, faster tool head speeds should also produce smaller feature sizes. For a given pressure, the mass flow rate of conductive material exiting the nozzle is constant. Equation 4.1 relates the mass flow rate ($\dot{Q}$) to the cross-sectional area of the deposited conductive trace (A_{cs}) and the toolhead speed ($V_{toolhead}$).

$$\dot{Q} = A_{cs} \cdot V_{toolhead} \qquad \text{Equation 4.1}$$

If velocity increases, the cross-sectional area will decrease. It is possible that this will cause the beads to become shorter, thinner, or both. The next section discusses the methods used to investigate this research question.

4.1.1 Experimental Method for Answering RQ1

In designing the experiment to assess the effects of the main factors (tip size, pressure, and tool head speed), it is assumed that there is no significant interaction between them. Each factor should affect Equation 4.1 independently. However there is no specific proof when considering PolyJet substrates. Thereby, a full factorial analysis is performed with each main factor combination on both PolyJet substrates VeroWhite+ and TangoBlack+.

Preliminary screening eliminated tip size as a main factor. It was observed that tips with a diameter smaller than 400 μm would clog repeatedly. At times, the metal particles clogged the nozzle to allow only the solvent portion of the ink to extrude. Therefore Table 4.2 only reflects the combinations of the main factors using the 400 μm tip diameter. For dispensing pressure, pressure under 31.03 MPa were not sufficient to extrude material and those over 41.81 MPa caused material agglomeration on the substrate surface and resulted in many discontinuities. When selecting toolhead speeds, the maximum is selected because of the X-Y motion system to accurately move faster. While extrusion at faster speeds is possible, it is not reliably so with the current setup. Beyond this speed barrier, there is expected to also be a physical limitation to toolhead speed based on the rheology of the conductive ink.

There are 18 different combinations in total shown in Table 4.2, and each combination is tested 4 times. For each factor combination, a 40mm long line is deposited onto one of the two printed substrates. Width data of the resulting deposited line is measured using a HIROX KH-7700 3D digital video microscope. Table 4.1 lists the range of main factors tested and the rationale for selecting those ranges. Table 4.2 shows the main factors tested.

Table 4.1: Selected main factor variable settings

Variable	Unit	Range	Rationale
Tip Size	[um]	[254-838]	Smaller tip sizes will produce finer features although there is a practical limitation where the conductive material will no longer extrude due to nozzle clogging. The selected range is also influenced by commercially available tip sizes for the pneumatic dispenser.
Dispensing Pressure	[kPa]	[31.03-41.81]	Equation 4.1 demonstrates that lower pressures will decrease the volumetric flow rate and thus lead to smaller features. Preliminary results show that pressures below 31.03 kPa are insufficient for extrusion. Pressure settings 37.92 and 41.81 kPa are also tested to observe potential interactions.
Substrate	[ ]	[VeroWhite+ , TangoBlack+]	These are the two main material for PolyJet printing. VeroWhite+ allows for rigid features, while TangoBlack+ is elastomeric and flexible.
Toolhead Speed	[mm/min]	[1000-3000]	Equation 4.1 demonstrates that faster toolhead speeds should also allow smaller features. 3000 mm/min is selected as an upper limit because the deposition machine is not capable of depositing reliably at faster speeds.

4.1.2 RQ1 Results

The average bead width data for each main factor combination is shown below in Table 4.3. Raw data from these experiments can be found in Appendix A. The highest pressure setting (44.81 kPa) induced nozzle clogging and resulted in discontinuous lines. As a result, width data is not gathered for that particular setting. For varying pressure, lower pressures exhibited thinner lines. In addition, faster toolhead speeds resulted in thinner lines. When comparing both substrates, lines written on TangoBlack+ were on average 343 μm thinner than those on VeroWhite+.

Table 4.2: Main factor combinations for Experiment 1

Trial Number	Dispensing Pressure [kPa]	PolyJet Substrate	Toolhead Speed [mm/min]
1	31.03	VeroWhite+	1000
2	31.03	VeroWhite+	2000
3	31.03	VeroWhite+	3000
4	31.03	TangoBlack+	1000
5	31.03	TangoBlack+	2000
6	31.03	TangoBlack+	3000
7	37.92	VeroWhite+	1000
8	37.92	VeroWhite+	2000
9	37.92	VeroWhite+	3000
10	37.92	TangoBlack+	1000
11	37.92	TangoBlack+	2000
12	37.92	TangoBlack+	3000
13	31.03	VeroWhite+	1000
14	31.03	VeroWhite+	2000
15	31.03	VeroWhite+	3000
16	31.03	TangoBlack+	1000
17	31.03	TangoBlack+	2000
18	31.03	TangoBlack+	3000

An ANOVA analysis of the main factors did not demonstrate any significant interactions, as shown by the interaction plot in Figure 4.1. The lines in these plots are mostly parallel and represent the different setting for the parameter listed in that row. It is possible that there may be a slight interaction between speeds and dispense pressures as the green and blue lines show some convergence.

The data for the explored parameter ranges fail to reject the hypothesis and indicates that as speed increases and pressure decreases, the line feature width decreases. On VeroWhite+, the smallest achievable trace was 879 µm and 720 µm on TangoBlack+. These values are highlighted in green in Table 4.3.

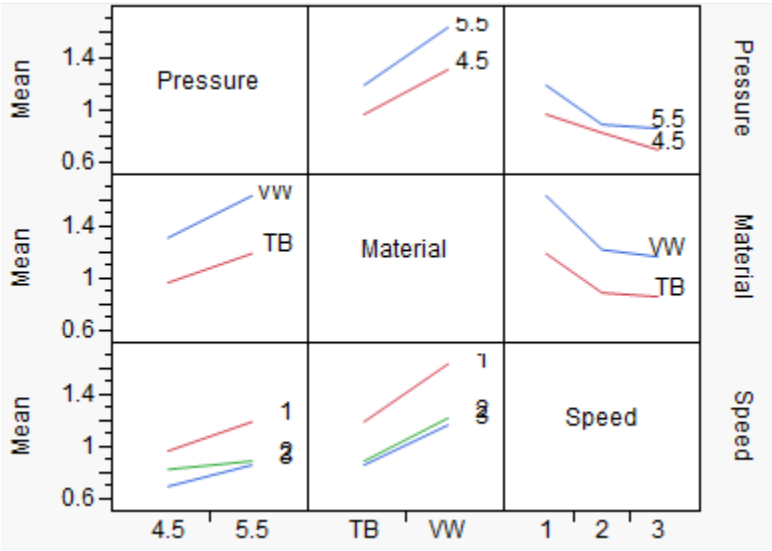

Figure 4.1: Interaction plots of average bead width between main factors

Table 4.3: Bead width data for main factor combinations

Trial Number	Dispensing Pressure [kPa]	PolyJet Substrate	Toolhead Speed [mm/min]	Average Width [mm]	Standard Deviation [mm]
1	31.03	VeroWhite+	1000	1.319	0.055
2	31.03	VeroWhite+	2000	1.070	0.045
3	31.03	VeroWhite+	3000	0.879	0.034
4	31.03	TangoBlack+	1000	0.957	0.062
5	31.03	TangoBlack+	2000	0.814	0.039
6	31.03	TangoBlack+	3000	0.720	0.069
7	37.92	VeroWhite+	1000	1.621	0.054
8	37.92	VeroWhite+	2000	1.206	0.131
9	37.92	VeroWhite+	3000	1.189	0.146
10	37.92	TangoBlack+	1000	1.200	0.049
11	37.92	TangoBlack+	2000	0.903	0.055
12	37.92	TangoBlack+	3000	0.837	0.112

4.1.3 RQ1 Discussion

This experiment shows that all of the main factors have an effect on the average feature width. The relationships that exist are:

- Increased pressure → Increase feature width
- Increased toolhead speed → Decrease feature width
- Feature width on TangoBlack+ **<** Feature width on VeroWhite+

If a consistent bead width is critical across the different substrates, the tool path could specify a change in toolhead speed to maintain consistency or adjust the dispense pressure. For example it is shown that dispensing on TangoBlack+ at 37.92 kPa and 2000 mm/min, the feature width is comparable to dispensing on VeroWhite+ at 31.03 kPa and 3000 mm/min. The bead width differs by only 24 μm on average. Additionally, this feature width data can be used to assist with designing channels into the PolyJet parts for encapsulation.

For all remaining experiments in this work, a dispense pressure of 31.03 kPa and a toolhead speed of 3000 are used since these settings yield the smallest feature sizes. While the bead height is not characterized in this section, it is measured in Section 4.3. The rationale is that these width measurements are taken before the ink is fully dry on the PolyJet substrate. Optical measurement indicated that the drying process does not affect the width, but the height changes considerably as the solvent evaporates. The next section discusses how different drying conditions affect the ink geometry. Once the drying process is better understood, height data is measured and discussed.

4.2 RQ2: How does drying time and temperature affect the geometry of conductive inks on PolyJet substrates?

The drying conditions of conductive inks are understood to have a positive effect on the conductivity and adhesion of conductive materials [46]. Given the motivation of creating functional circuitry, high conductivity and strong adhesion is desirable. Commercially available conductive inks are prescribed a drying regimen of specific temperature and duration for ensuring quality conductivity and adhesion. It is recommended by the supplier to cure the DuPont 5021 ink at 120°C for at least 5 minutes [46]. However, these temperatures are in

excess of the PolyJet material's glass transition temperatures (54°C) and, therefore, not compatible.

This research question aims to explore how varying dry times and temperatures (compatible with PolyJet material) affect the final conductivity and adhesion of silver-loaded conductive ink on PolyJet substrates. In addition, the height of dried lines is analyzed to determine if the narrower lines observed on TangoBlack+ versus VeroWhite+ substrates (Section 4.1) result in taller features.

Initially, it is hypothesized that drying the ink at temperatures near the published glass transition temperatures of the PolyJet materials will not significantly impact adhesion and profile geometry of the conductive traces. It is observed that as the deposited beads dry, the cross-section settles and shrinks in the Z-direction as the solvent evaporates. Rapid drying could potentially inhibit this settling effect and cause different cross-sectional profiles than specimens dried over a longer period of time at room temperature. If the geometry is not significantly affected, the heated drying regimen can be used as higher temperatures help the ink cure faster.

4.2.1 Experimental Methods for Answering RQ2

The experiment outlined in this section is designed to investigate the effects of drying time and temperature on the geometry of the conductive traces on the PolyJet substrate. In order to understand the potential effects on adhesion on the cross-sectional geometry, contact angle and bead height are measured. Two sets of samples were evaluated: (i) samples that are allowed to dry in air for 24 hours and (ii) samples that are dried at 55 °C for 30 minutes (which is near the material's heat deflection temperature).

Because the goal is to encapsulate the directly written traces after deposition with subsequently printed layers, the components cannot be removed from the build tray and treated in an oven. Removing the components would require them to be replaced on the build tray with microscale precision. Instead, a heat gun is used to force warm air over the samples during the drying process on the build tray. 3-dimensional profilometry is used to determine if there is any significant change in the cross-sectional profile between the two sample sets.

A HIROX Digital Video Microscope is used to capture 3D profilometry data. The microscope uses a composite of multiple images with different focal planes to construct a 3D profile as shown in Figure 4.2. From the 3D profile, cross-sectional profile and height data is made available.

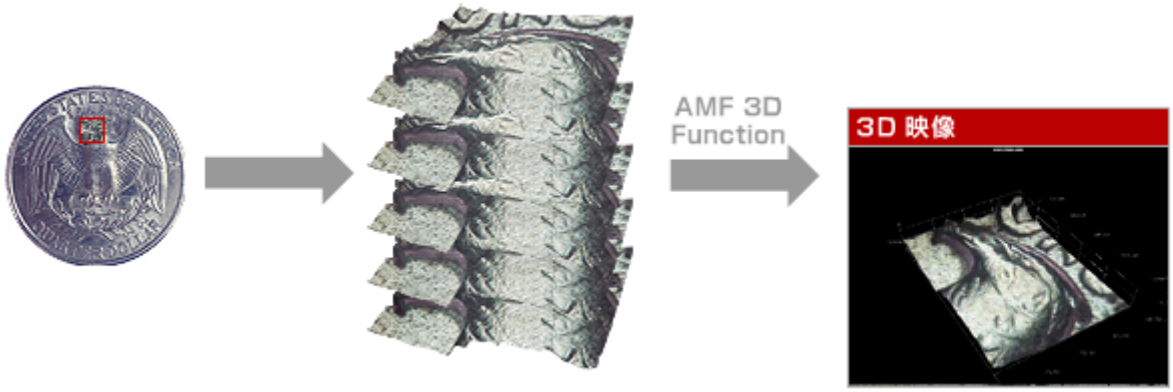

Figure 4.2: Demonstration of HIROX multi-focus 3D synthesis process used under fair use, 2013[47]

For this experiment, conductive traces were deposited on the surface of the PolyJet VeroWhite+ and TangoBlack+ substrates using the dispense parameters determined in Section 4.1. The dispense pressure was set to 31.03 kPa (4.5 psi) and the toolhead speed was 3000 mm/min using a 406 µm diameter dispensing tip. Once the traces were deposited, small sections were selected to view under the microscope. A demonstration of where the microscope is focused is shown in Figure 4.3.

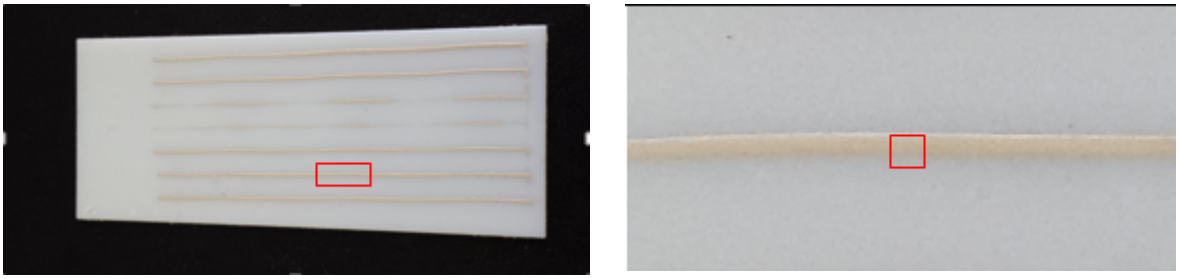

(a) **(b)**

Figure 4.3: Demonstration of sample profilometry location

In Figure 4.4, topographical data of only half the bead is visible because at the magnification necessary to gather 3-dimensional data from different focal planes the field of view is limited. However, it is assumed that the bead's profile is symmetric. Using the HIROX multifocal synthesis, a 3D model is constructed as shown in Figure 4.4.

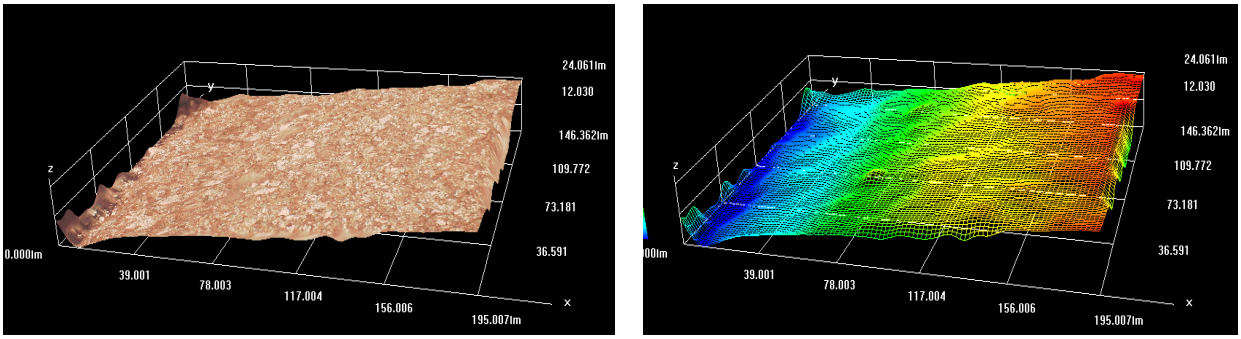

(a) **(b)**

Figure 4.4: 3-dimensional model using HIROX multi focal synthesis with (a) actual image data overlaid and (b) a colored surface for indicating relative height.

4.2.2 RQ2 Results

Using many 3D models, maximum height data was taken for the different samples that underwent room temperature drying and heated drying on both TangoBlack+ and VeroWhite+ substrates. The recorded data is tabulated in Table 4.4 and shows only a small difference in the observed average heights. On the samples without any sort of heat treatment, the heights averaged to be 27 and 36 μm on VeroWhite+ and TangoBlack+ respectively. With heat treatment, there was very little change. The average heights were 28 μm on VeroWhite+ and 38 μm on TangoBlack+. It is possible that the accelerated evaporation of the solvent caused a more porous final conductor that is taller. As the solvent from the center of the trace began to volatize and escape, it encouraged porosity between the particles.

Using a simple t-test, assuming a two-tailed distribution and an alpha of 0.05, a p-value of 0.583 is given and we cannot conclude a significant difference in geometry between the drying methods on either TangoBlack+ or VeroWhite+. The accelerated drying conditions do not significantly affect the profile geometry of the conductive materials to the PolyJet substrate.

Table 4.4: Tabulated height data for samples (i) heated at 55 °C for 30 minutes and (ii) air-dried for 24 hours

Sample	Heat Treatment	Height [um]		Average [um]	Standard Dev. [um]
		VeroWhite+	TangoBlack+		
1	Y	26.06	38.55	VeroWhite+	
2	Y	27.66	37.48	**27.513**	**0.919**
3	Y	28.39	37.86		
4	Y	26.94	37.32	TangoBlack+	
5	Y	28.51	37.36	**37.714**	**0.459**
6	N	26.17	35.45	VeroWhite+	
7	N	31.41	36.17	**26.758**	**2.548**
8	N	24.06	36.22		
9	N	27.14	35.93	TangoBlack+	
10	N	25.01	37.14	**36.182**	**0.551**

4.2.3 RQ2 Discussion

This experiment shows that the heating process, which helps the ink dry faster, does not significantly impact the final geometry of the deposited features. There is no information from the supplier that indicates temperatures below the recommended curing temperature will have any positive impact on the final conductivity [46]. The heat applied is to reduce the drying time before printing can be resumed. The height of the traces after heating is also of interest because it can influence the decision to design channels for embedding the material. Traces on VeroWhite+ are shorter than 32 μm, which is the layer height of the PolyJet process. Traces on TangoBlack+ are only 5 μm taller than the PolyJet layer height on average. Because of this, channels should be designed to be 32 μm deep as the PolyJet process would not be able to accommodate shallower features.

Returning to RQ1 regarding profile geometry, we also notice a difference in heights between the VeroWhite+ and TangoBlack+ features. Recalling Equation 4.1, we know that if the features are narrower, than the height should also be taller. This relationship is confirmed by these results. Conductive features on TangoBlack+ are taller and narrower than those on

VeroWhite+. This effect is possibly related to adhesion or surface interaction of the conductive materials to the PolyJet substrates and is explored in answering Research Question 3.

4.3 RQ3: What are the adhesion characteristics between the conductive ink and PolyJet substrates?

The advantages of embedding conductive elements within a part have been discussed (Section 1.2); however, the embedding process does prevent the servicing of these conductive traces after manufacture. After manufacture, the conductive traces may be completely inaccessible. An internal connection failure or physical break in the conductive trace could render the component nonfunctional. In order to ensure reliable connections, it is important to understand the adhesion characteristics between the conductive materials and the PolyJet substrates. When not bonded to a surface, the thin conductive traces are prone to breaks from movement or vibrations. However, when the conductive material is able to bond to a surface, the traces are constrained and less susceptible to breaks. Good bonding between the conductive material and PolyJet substrate creates stable traces and thus reliable connections. Poor bonding, results in suspended traces that are more susceptible to cracking and failure.

Material wetting is a fair indicator of inter-material adhesion [48]. Material wetting is defined as how well a liquid phase material contacts a solid surface on a molecular level and is a result of interaction of cohesive and adhesive forces. Young's equation (Equation 4.2) effectively models the scenario of a fluid droplet on a solid surface by relating solid-liquid free energy (γ_{sv}), solid-surface free energy (γ_{sl}), and liquid-surface free energy (γ_{lv}) to the droplet's contact angle.

Materials with contact angles below 90° are considered hydrophilic and exhibit a strong solid-liquid interaction. This interaction provides ample contact between the liquid and solid for adhesion. The experiments designed to answer RQ3 aim to measure the contact angle to determine if the conductive inks adhere well to the PolyJet substrates.

$$\gamma_{sv} = \gamma_{sl} + \gamma_{lv} \cos\theta$$ Equation 4.2

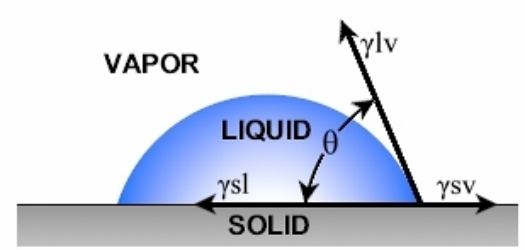

θ = Contact Angle

γ_{lv} = liquid-surface free energy

γ_{sl} = solid-surface free energy

γ_{sv} = solid-liquid free energy

Figure 4.5: Diagram of Young's equation variables

4.3.1 Experimental Methods for Answering RQ3

Sample pieces of VeroWhite+ and TangoBlack+ substrates were printed and droplets of the conductive material were applied. The droplets were semi-manually applied to the substrate using a discrete 0.25 second extrusion dosage from the Nordson EFD pneumatic dispenser, as shown in Figure 4.6. In order to measure the contact angle, a digital microscope was positioned parallel to the adhesion surface and the sample was backlit in order to create a silhouetted droplet as shown in Figure 4.7. Using the images captured by the microscope, the contact angle was digitally measured via ImageJ measuring software. A sample image is shown in Figure 4.8. Finally, scotch tape is applied and removed to the dried sample to see if any material is removed to test adhesion strength.

Figure 4.6: Droplets produced by 0.25 second dispensing pulses on VW substrate

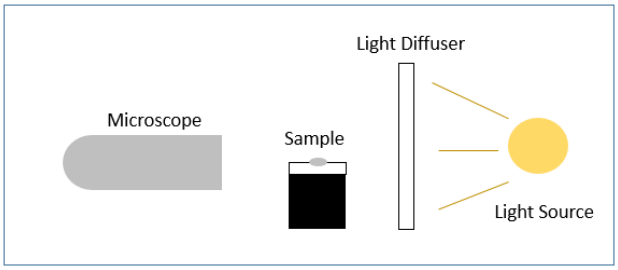

Figure 4.7: Contact angle measurement setup schematic

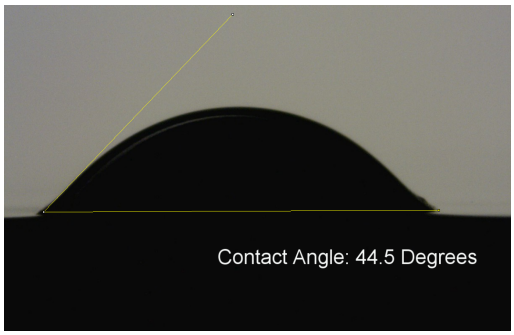

Figure 4.8: Example of ImageJ digital measuring process

4.3.2 RQ3 Results

The resultant contact angle measurements are presented in Table 4.5. Droplets on the VeroWhite+ substrates had an average contact angle of 31.6 degrees with a standard deviation of 2.7 degrees. The TangoBlack+ samples had an average of 37.7 degrees with a standard deviation of 3.2 degrees. Both of these averages are well within the hydrophilic range and demonstrate good wettability and adhesion. Moreover, no material was removed from either substrate using the scotch tape test. When adhered and removed, no material was visibly resent on the surface of the tape.

As hypothesized from observations in RQ1 (Section 4.1), the conductive material on the TangoBlack+ surfaces averaged a larger contact angle, which would imply that the lines are thinner for a constant cross-sectional area. An example of the VeroWhite+ and TangoBlack+ profiles that demonstrate these differences are shown in Figure 4.9.

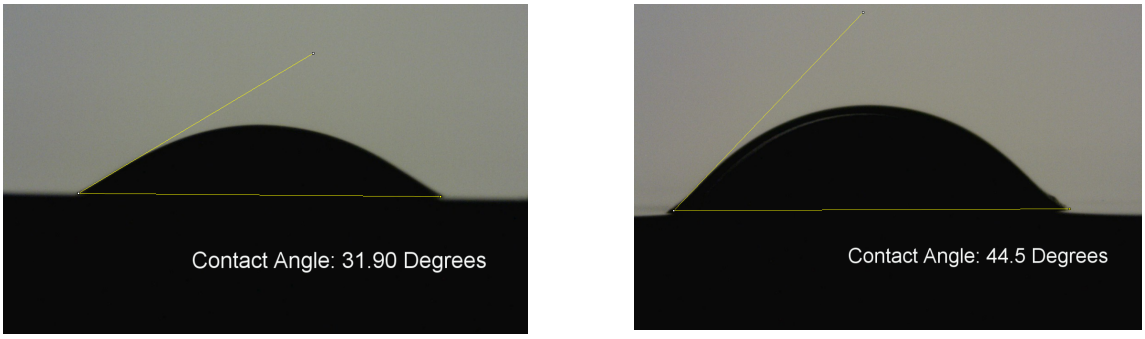

(a) VeroWhite+ (b) TangoBlack+

Figure 4.9: Comparison of contact angles on (a) VeroWhite and (b) TangoBlack substrates

Table 4.5: Contact angle measurements

	Contact Angle [°]	
	VeroWhite	TangoBlack
1	31.9	33.74
2	33.2	36.99
3	34.7	40.02
4	35.15	39.47
5	32.82	36.3
6	31.12	35.4
7	31.59	44.5
8	30.54	39.75
9	30.22	36.18
10	25.33	35.04
Average	**31.66**	**37.74**
Std. Dev.	**2.77**	**3.2**

4.3.3 RQ3 Discussion

The contact angle results supports the reasoning as to why features on TangoBlack+ are thinner than on VeroWhite+ as discovered in RQ1 (Section 4.1). Given that both average contact angles are well within the hydrophilic range, good adhesion is expected on both substrates, although adhesion to VeroWhite+ is relatively better (as per the smaller contact angle). Additionally, ink on both substrates passed the “scotch tape test.”

While using the HIROX digital video microscope during the experiments for RQ2 (Section 4.2), it was observed that the PolyJet material surfaces (both VeroWhite+ and TangoBlack+) had many small imperfections or divots on the surface as shown in Figure 4.10. It is unclear what causes the small holes, but it may be attributed to inkjet head misfires, imperfections in the roller, or adhesion to the roller. However, these holes may also play an important role in the conductive materials’ adhesion to the PolyJet surface on the macro scale by allowing the material to penetrate and gain more surface area for adhesion.

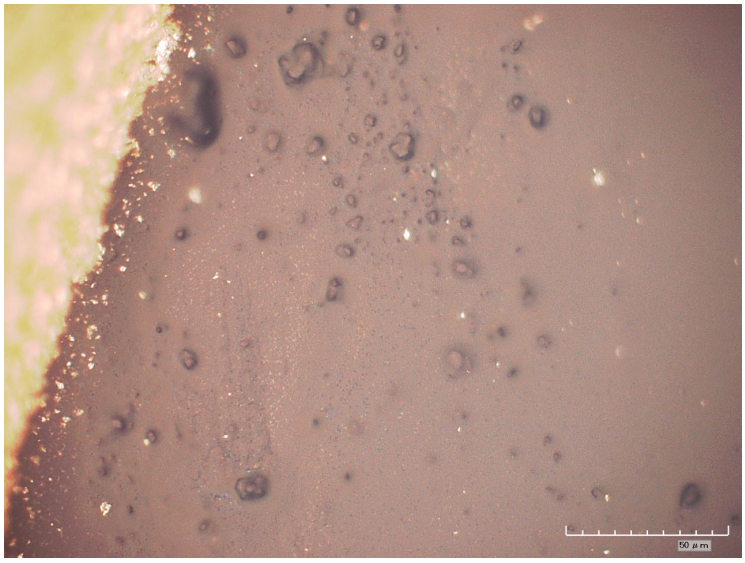

Figure 4.10: Microscope image of surface imperfections on TangoBlack+ substrates.

4.4 RQ4: How does embedding and encapsulation affect conductivity of directly written conductors?

When depositing conductive traces on an additively manufactured component, the material can be deposited on an outside facing surface, or it can be fully embedded and encapsulated by subsequently printed layers. Encapsulating conductive traces is critical for enabling truly embedded electronics and sensors in components. Until now, our conductive materials have only been deposited on the substrate surface. This research questions aims to discover if the DuPont 5021 conductive material remains conductive when encapsulated and if so, to what degree.

To demonstrate the different possible methods of encapsulation, four different substrate/trace configurations are shown in Figure 4.11:

1. In the first configuration, a conductive trace is deposited on the substrate surface with no encapsulation. This is a datum for traces printed on the PolyJet surface.
2. In the second configuration, conductive material is deposited on the surface and is then printed over with subsequently printed layers. The printing and rolling steps discussed in Section 1.1 are thought to deform the conductive trace, however the effects of this are not known for sure.

3. The third configuration, is also encapsulated; however, a channel is printed into the surface so that the deposited trace is recessed and level with the build surface before resuming the print. The channel geometry is designed with the cross sectional profile geometry found in Experiments 1 and 2 using the average bead width and height.
4. The final configuration is similar to the third in that an empty channel is designed for conductive material although the walls of the channel are not printed until after deposition.

Configuration 1 is used as a datum for determining the conductivity of traces that are deposited on the surfaces of PolyJet substrates. Configuration 2 encapsulates conductive traces written on the surface on a PolyJet substrate. It is hypothesized that the leveling roller may compress the conductive trace and negatively impact conductivity. Configuration 3 includes a subsurface channel for the deposited trace that protects it from the PolyJet roller. Configuration 4 is similar, although the channel is printed after the conductive trace is deposited.

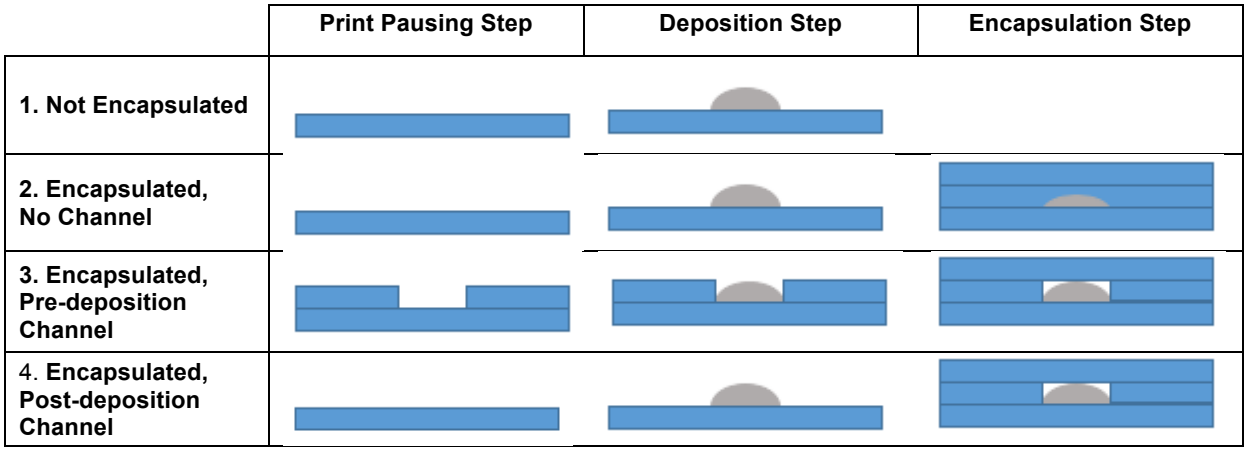

Figure 4.11: Process flow description of different direct write encapsulation methods in a layer-by-layer build process

4.4.1 Experimental Methods for Answering RQ4

In this experiment, five traces are printed on TangoBlack+ and VeroWhite substrates using configurations 1, 2 and 3 from Figure 4.11, and the conductivity is measured. Configuration 4 is not included because it almost identical to Configuration 3, although the channel is not visible during the deposition step. Configuration 3 is more practical because it is visible during the

deposition step and the direct write system can be aligned accordingly. In total, there are six different configurations each with five traces, resulting in 30 data points.

In experiments using Configuration 3, conductive material is deposited into predefined channels on a PolyJet substrate and then encapsulated as shown in Figure 4.12. The channels are designed to be one layer (32 μm) tall since the average bead height measured from the 3-dimensional profiles were 27 μm and 38 μm tall on VeroWhite+ and TangoBlack+, respectively (Table 4.4). The encapsulated specimens were printed using a “zero support material” configuration so that no support material would need to be removed from the channel before the direct write process. The “zero support material” configuration disables the automatic deposition of support material under overhangs by the PolyJet process. After the conductive material is deposited and dried using the same heat treatment as in Section 4.2 (30 minutes at 55 °C), the print was resumed to fully encapsulate the conductive materials as illustrated in Figure 4.11. The final part is shown in Figure 4.12. Conductivity is indirectly measured by resistance, which is inversely related.

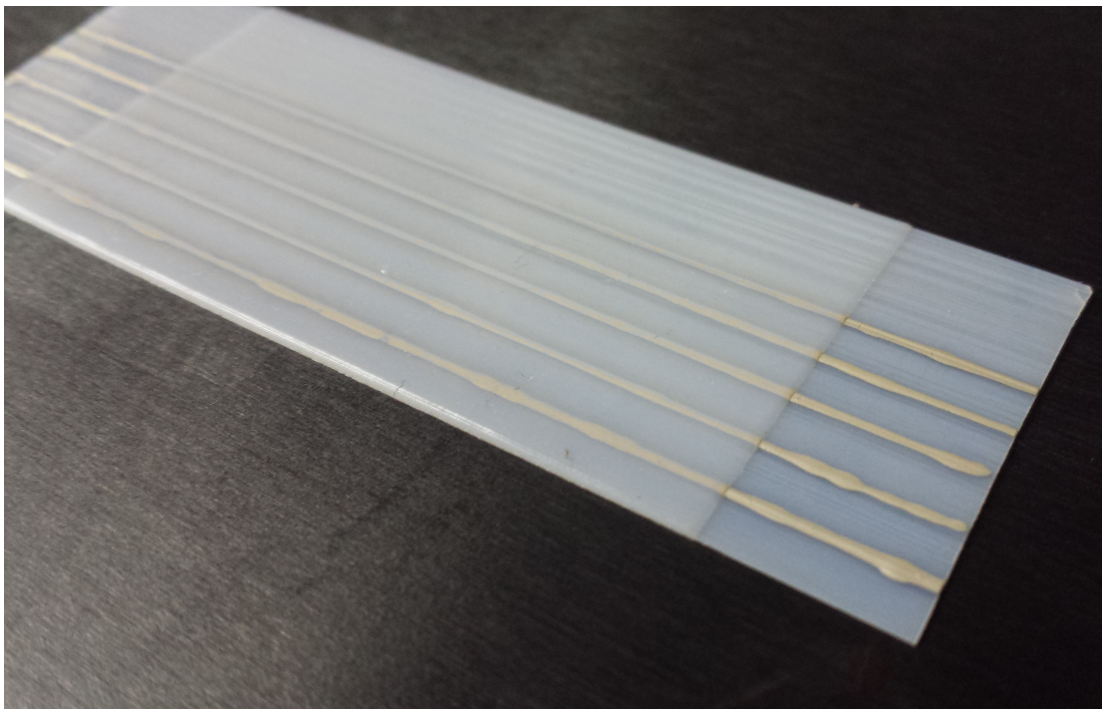

Figure 4.12: Conductive traces fully encapsulated in printed part. The end portions are left exposed for measurement purposes.

4.4.2 RQ4 Results

From this experiment, traces deposited on the substrate surface (configuration 1, Figure 4.11) are found to be more conductive than any of the encapsulated traces. The raw and average data for both VeroWhite+ and TangoBlack+ substrates is given in Table 4.6. The averages are listed for each configuration. The data in yellow is calculated from only the VeroWhite+ data, while the data in green represents the measurements from TangoBlack+.

Table 4.6: Resistivity measurements for different encapsulation configurations

	Resistance [Ω]		Average [Ω]	Standard Deviation
	VeroWhite+	TangoBlack+		
Configuration 1	0.669	2.201	**1.357**	**0.427**
	1.133	1.584	**VeroWhite+ Only**	
	1.480	1.019	1.209	0.312
	1.551	0.941	**TangoBlack+ Only**	
	1.212	1.776	1.504	0.473
Configuration 2	29.1	29.3	**27.4**	**3.5**
	28.0	32.6	**VeroWhite+ Only**	
	28.7	25.4	27.6	3.1
	21.6	27.7	**TangoBlack+ Only**	
	30.5	21.2	27.2	3.8
Configuration 3	27.2	22.0	**24.9**	**4.5**
	20.1	35.2	**VeroWhite+ Only**	
	22.7	30.1	23.0	2.4
	21.3	21.3	**TangoBlack+ Only**	
	23.8	25.6	26.8	5.2

The average resistance of conductors deposited on the surface is 1.357 Ohms, while those encapsulated using Configurations 2 and 3 had an average resistance of 24.9 and 27.4 Ohms, respectively. Using t-tests to compare Configurations 2 and 3 to Configuration 1, data suggests a statistically significant difference between embedded and non-embedded conductors. Encapsulation demonstrates lower conductivity, possibly by inhibiting further drying or curing of the conductive traces once encapsulated from the open atmosphere. The p-values calculated between the different cases do not exceed 4.05E-5 which is lower than an alpha of 0.05. While the average values for Configuration 2 (encapsulated with no channel) are higher than

Configuration 3, a t-test fails to conclude any statistically significant difference between the TangoBlack+ substrates with a p-value of 0.74. When comparing the VeroWhite+ substrates made with configurations 2 and 3, the p-value (0.047) is slightly lower than the alpha of 0.05, suggesting a significant difference between the two. The substrate with a channel designed for embedding showed improved conductivity over those without channels on VeroWhite+ but not TangoBlack+.

4.4.3 RQ4 Discussion

In this experiment, encapsulated traces are shown to be less conductive than those deposited on the surface. The use of recessed channels does not seem to alleviate the issue. The hypothesis suggested that the PolyJet roller could be responsible for any change in conductivity although this is not the case. The reduced conductivity may be a result of a chemical or physical interaction between the PolyJet photopolymer and the conductive material; however, this has not been documented before in previous works that used conductive metals inks with photopolymer substrates [9], [13], [21]. Comparisons using the same DW process on a known non-reactive substrate would be needed to assess this.

Another potential cause for this drop in conductivity is post-print drying or curing at room temperature. The traces deposited on the surface maintain a large exposed surface area for continued drying at room temperature as the printing process finishes. The encapsulated traces however are sealed from the external environment and thus prevent drying any further. It is suggested for future work to assess longer drying cycles to investigate this effect.

For VeroWhite+ substrates, channels designed for depositing conductive material are shown to improve conductivity. Channels are less important for traces written on TangoBlack+ substrates. This difference is most likely due to the differing material properties of the two substrates. As the PolyJet roller passes over traces on VeroWhite+ material, the traces are pressed against a rigid substrate causing the traces to deform and become more resistive. TangoBlack+ substrates, however, most likely deform under the roller before the traces do. Instead, the traces are impressed into the TangoBlack+ substrates and retain their original shape. However, the encapsulated traces in both cases are less conductive than traces on the substrate surface. Nonetheless, the encapsulated traces do remain conductive and continuous

through the encapsulation process. Chapter 5 will describe the potential applications of these embedded conductors.

5 POTENTIAL APPLICATIONS OF HYBRIDIZED DIRECT WRITE AND POLYJET TECHNOLOGIES

In the previous Chapters, a direct write system capable of dispensing DuPont 5021 conductive silver ink is designed for integration with the PolyJet process. The machine is capable of depositing 700 μm wide lines that are 32 μm tall (Section 4.1.2). The lines are written and dried on PolyJet substrates using heat to speed the process (Section 4.2). It is discovered that when traces are encapsulated with the PolyJet process, conductivity is impacted negatively (Section 4.4). The average conductivity for deposited traces on the surface is 1.4 Ω, and 27 Ω when encapsulated. Because of this high resistance, these lines are not suited to carry currents for high power applications, such as powering motor or batteries. However, this section explores low-power sensing applications that the traces are particularly well suited for, such as in-situ strain sensing (Section 5.1) and capacitive sensing (Section 5.2).

5.1 In-Situ Strain Sensing

Strain gages measure the strain of an object using a series of conductive traces aligned parallel to the direction of the strain applied. The strain is indirectly measured by a change in resistance of the conductors as they deform. Typically, strain gages are affixed to manufactured components using adhesive. Direct write and component embedding allow for these strain sensors to be directly manufactured into a component's internal structure. This not only allows for the circuitry to be protected; it also allows for continuous and uninterrupted external surfaces, which is particularly important for aerospace applications.

5.1.1 Strain Gage Exploration

As a proof of concept, traces were encapsulated in VeroWhite+ substrates to measure deflection (as shown previously in Figure 4.12). Using a digital multimeter set to measure resistance, no change is initially observed; however, the sensitivity of the multimeter is only 0.1 Ohm. Any resistance change below 0.1 Ohm is therefore undetectable by the multimeter alone. Using an external power supply and a Wheatstone bridge, small changes in resistance can be indirectly measured by a change in voltage. This setup allows one to observe a measurable change in voltage when the encapsulated trace is deflected. As shown in Figure 5.1, the voltage difference drops from 683 mV to 676 mV when the part is deflected. While this is a small

change, this experiment is merely a demonstration that there is a detectable change. Finer tuning of the Wheatstone bridge and amplifying the output potential would enable better resolution in detecting deflection.

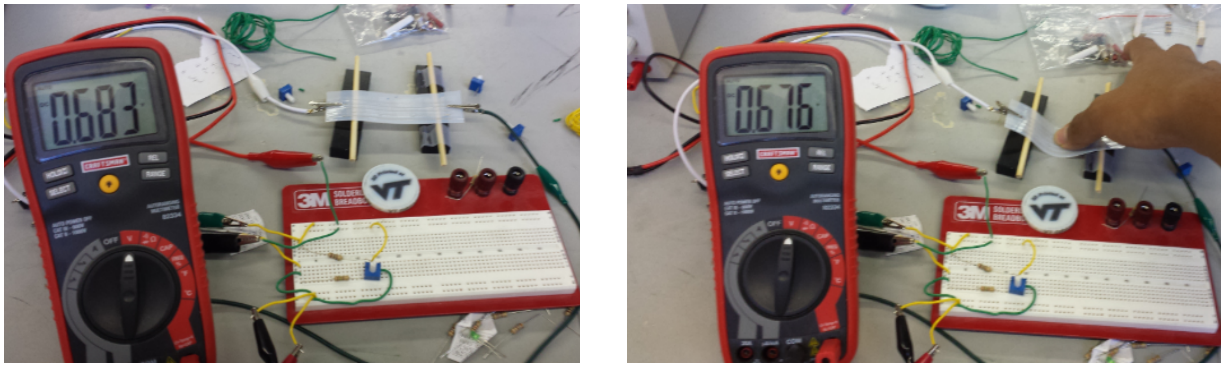

(a) **(b)**

Figure 5.1: Change in voltage as a result of part deflection

To further our understanding of how deflection or strain can be measure with directly written conductors, strain gage-like geometry is deposited and encapsulated in a TangoBlack+ component, which is very flexible. As the substrate is deformed, the conductor should also deform and this can be measured by a change in resistance. To aid with the careful observation of the printed strain gage's performance, the samples were placed over curved forms (printed using Fused Filament Fabrication) with varying radii of curvature (40-90mm). Resistance measurements were taken over each form, as shown in Figure 5.2. The results are shown in Figure 5.3. The results show a general trend of increasing resistance as the deflection increases. These embedded strain sensors may be used to provide feedback in applications where deflection sensing is needed on continuous surfaces such as flexible control surfaces.

A concern with strain sensing is the mesostructure of the directly written conductor. Conventional strain gages are made of near-fully dense conductors. As they are strained, their cross-sectional area changes and causes the resistance to increase. The deposited conductors are comprised of many individual metal particles. It is possible that the metal particles shift as the traces are strained and introduce non-linearity in the sensor's response potentially indicated

by the dip between 60 mm and 70 mm radii of curvature in Figure 3.5. While sintering may not be possible to create a bulk conductor, there may be a theoretical cross-sectional area which provides enough particle-to-particle contact at all times to mitigate the error cause by the shifting or particles during deflection. This theoretical area is likely a function of the mean particle diameter and particle density although its assessment is considered future work.

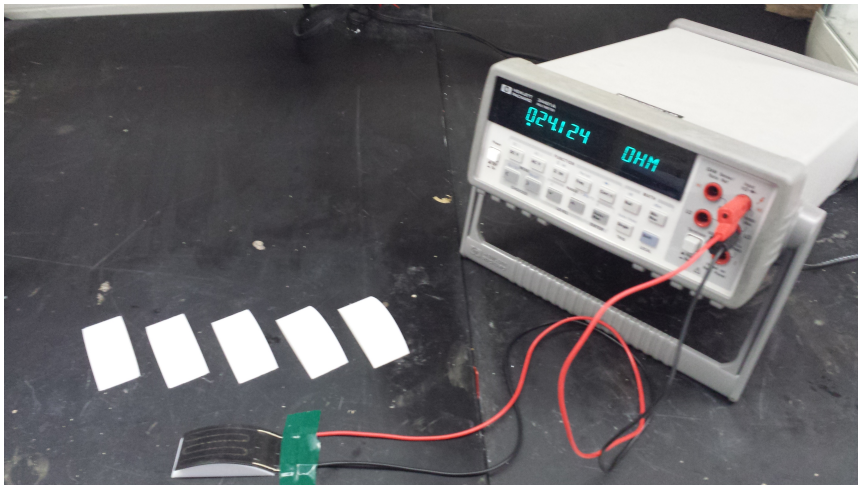

Figure 5.2: Experimental setup for testing change in resistance as a function of deflection

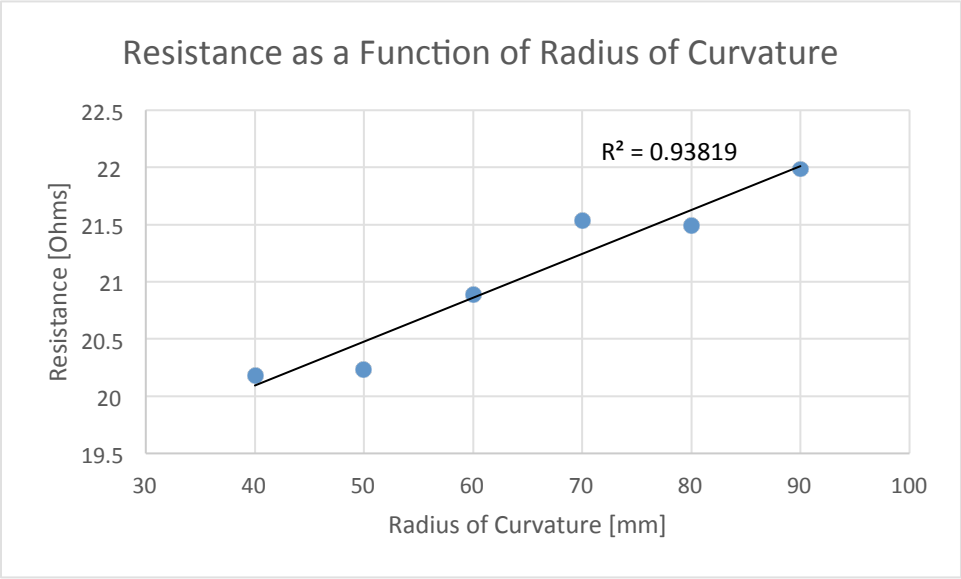

Figure 5.3: Resistance of directly written silver traces as a function of radius of curvature

5.1.2 Embedded Actuation and Strain Sensing on Flexible Control Surfaces

Flexible control surfaces are defined as “hinges that work based on the flexion of material in the hinge, rather than having a bearing of some sort”[8]. Living hinges have the advantage of being of single piece construction so there are no interfacing or connecting junctions which are sites of failure. Because of the PolyJet’s ability to print both rigid and elastomeric materials, these continuous flexible control surfaces can be manufactured.

In the context of remotely-piloted aircraft (RPA) wings, flexible control surfaces can provide a continuous member with no gaps, and thus allow unobstructed fluid flow over the wing. Previous work has shown that these types of flexible control surfaces, in contrast to rigid control surfaces, produce more lift with less drag (Figure 5.4) [49]. Leveraging additive manufacturing and component embedding, it has also been demonstrated that the flexible control surfaces can be actuated using fibrous “tendons” [50]. Moreover, the addition of strain sensing circuitry could provide closed-loop control to such an actuation system. By combining direct-write of conductive materials and the component embedding process with PolyJet manufacturing technology, closed-loop sensing of control surface actuation is possible.

Type	Drag force (mN)	Drag coefficient	Lift force (mN)	Lift coefficient	Moment (mN·m)	*Re*
Rigid control surface	15.9	0.0135	15.9	0.026	0.68	9000
Flexible control surface	14.1	0.0109	16.7	0.027	0.938	13000

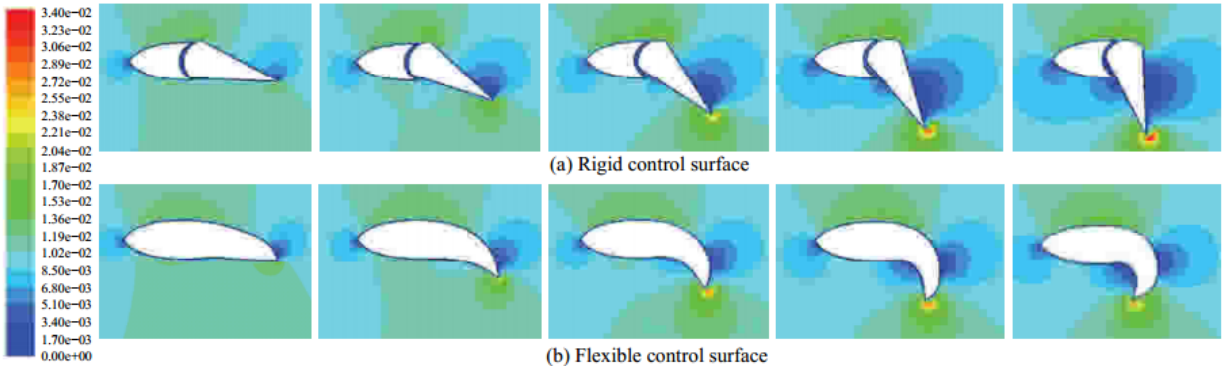

Figure 5.4: Flow visualization, lift coefficient, and drag coefficient comparisons between rigid and flexible control surfaces used under fair use, 2013 used under fair use, 2013[49]

The following component in Figure 5.5 is a hydrodynamic airfoil section that implements a flexible control surface. The structure is fabricated using the PolyJet process. The main

structure is printed using VeroWhite+ and the joint connecting the trailing flap to the main body is made of the flexible TangoBlack+ material. The airfoil contains embedded shape memory alloy (SMA) strands for actuation and directly written conductors for deflection sensing. Springs are also used to supply a bias force for returning the wing to its neutral position. When current is applied to the SMAs, heat is generated, causing the strands to contracts. The axial contraction pulls the trailing flap down. When the current is removed, the bias force from the springs returns the flap to its neutral position.

Through the TangoBlack+ section, a series of conductive traces are written to sense the deflection. The embedding plane and trace geometry is shown in Figure 5.6. In the neutral position, a resistance of 9.822 Ohms is measured. When fully deflected, a resistance of 10.079 Ohms is measured. This application demonstrates the ability to combine embedded sensing and actuation in PolyJet components leveraging the ability to fabricate continuous and compliant flexible control surfaces. The embedding sensing could be further leveraged to provide closed loop control of the actuation system.

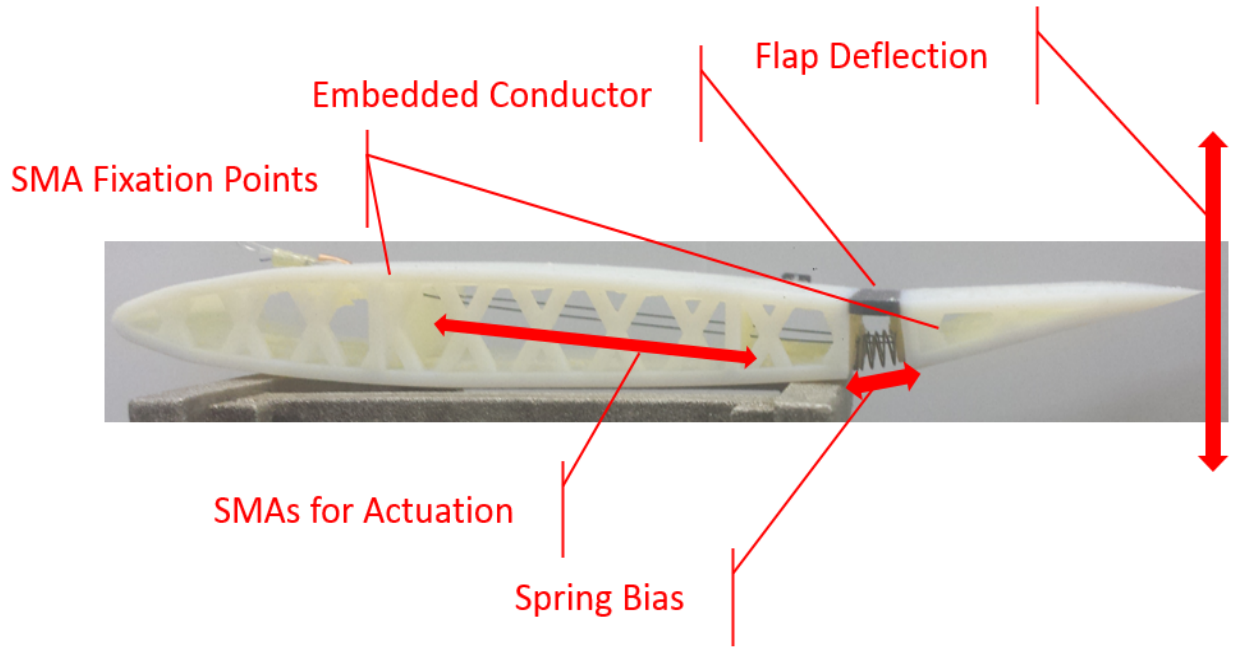

Figure 5.5: Airfoil with embedded actuation and sensing using SMAs and directly written conductors.

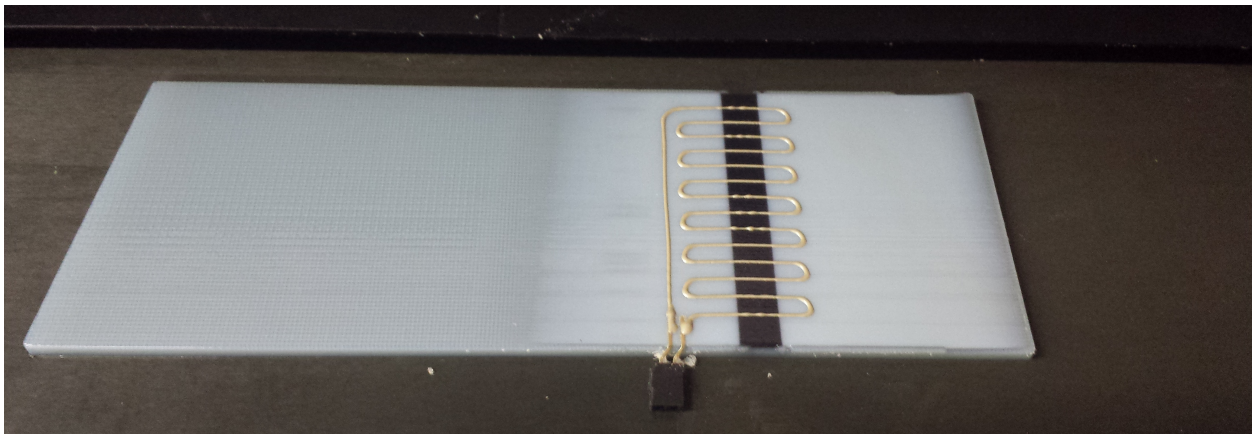

Figure 5.6: Embedding plane and geometry of directly written conductor shown on PolyJet build tray during the mid-print deposition step.

5.2 Embedded Capacitive Sensing

Capacitive sensing has found commercial applications in various areas such as fingerprint scanning, touchscreen technology, and other contactless sensing. Capacitive sensing detects a change in capacitance when a conductor is moved near the sensor. The sensor in construction is simple and can be made with any conductive material including conductive ink. A single trace can be used as a capacitive sensor. A more sensitive sensor can be made by directly writing a conductor with a larger surface area. Unlike the strain sensors, capacitance sensors do not need to be strained or touched to register feedback. Because capacitive sensing is contactless, the conductors can be fully embedded and protected from external conditions.

Using an Arduino microcontroller with the “Cap Sense” library, capacitance changes were detected from directly written conductors (individual lines). Using the Cap Sense library, sensing pins were connected to directly written traces. The component in Figure 5.7 also feature embedded header pins for connecting to external circuitry. The serial monitor shown in Figure 5.8 is the Arduino registering data from the capacitive sensor. The left column is the data point number and the right column is the capacitance value. Higher values indicate a conductor is near. With no conductors near, values of 0-45 are reported. When a hand is brought within 1 inch of the conductive trace, the values increase to near 1000 as shown in Figure 5.8.

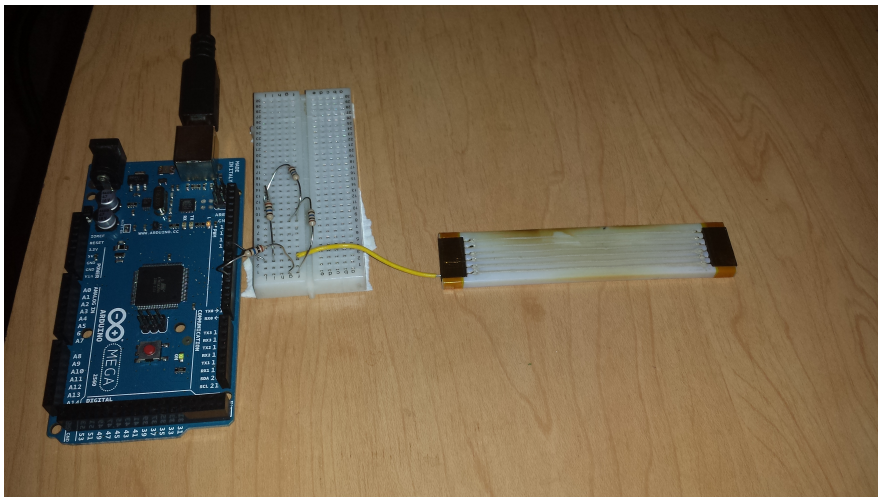

Figure 5.7: VeroWhite+ component with directly written connectors.

Capacitive sensors can be used to measure many different types of data including pressure, proximity, and fluid flow using the basic principles shown here. This simple demonstration shows how these sensors can be made with directly written conductors and potentially embedded into PolyJet manufacture components. Future work will assess the capability of capacitive sensors that are fully embedded in PolyJet substrates and correlate capacitance values to actual distances. This demonstration is solely a proof of concept for using directly written conductor on PolyJet substrates as capacitive sensors.

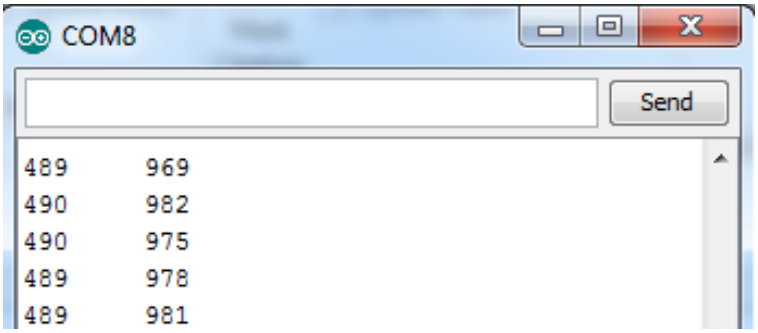

Figure 5.8: Serial monitor receiving values from Arduino as capacitance changes. The left column is the data point number and the right column is the capacitance value. Higher values indicate the presence of a conductor.

6 CONCLUSIONS AND FUTURE WORK

6.1 Summary of Research

The primary goal of this work was to develop a process to directly manufacture embedded electronics within PolyJet components during part fabrication. This goal has been achieved by designing and building a system that can be inserted into the PolyJet machine to dispense conductive silver ink onto a part via an extrusion-based, high precision fluid dispenser. An extrusion system was selected because of its ability to deposited heavily loaded conductive inks. DuPont 5021 silver-loaded ink is selected because of its high metal density and the corresponding achievable as-deposited conductivity without post-process sintering (which is amenable to the low deflection temperatures of the PolyJet polymers). The tool head is mounted to an X-Y stage specially designed to fit in the PolyJet machine and is controlled using standard g-code. A video-based calibration system is designed to compensate for coordinate system offsets between the PolyJet and direct write systems.

With respect to the developed customer needs, the machine adequately meets all needs, with the exception of target resolution. The machine is highly automated and is able to deposit material on the PolyJet build tray without interfering with the PolyJet process. The minimum feature width (700 μm) is considerably larger than the 42 μm target. The 700 μm limit is largely a function of the smallest usable tip diameter before clogging. Smaller features may be possible with more sophisticated extrusion based technologies, such as micropump dispensing.

The key considerations for combining direct write with PolyJet technology were established from reviewing previous works that combine direct write with other additive manufacturing process. These considerations include:

- Without post process sintering, heavily loaded metal inks are desired to provide the best conductivity.
- Direct write technology selection is primarily based on material viscosity, deposition resolution, deposition thickness, and motion control complexity requirements.
- Multilayer conductors are difficult due to the need to replace and remove the direct write system at every layer.
- Good adhesion between the conductive material and PolyJet substrate is critical.

In addition to the development of a system, four Research Questions were investigated to understand the effects of the system's process parameters on the quality of the resultant part.

Research Question 1: How do tip size, dispense pressure, and tool head speed affect feature width?

Identifying important process parameters for depositing and drying conductive inks was critical for developing an embedding process for directly written conductors. DuPont 5021 ink was deposited using an extrusion-based, high precision fluid dispenser through a 400 μm diameter nozzle at various toolhead speeds and dispense pressures. Lower pressures and higher toolhead speeds were found to produce the smallest features. Conductive traces as small as 700 μm wide and 36 μm tall were able to be dispensed by the system (Section 4.1.2).

Research Question 2: How do drying time and temperature affect the geometry of the conductive inks on PolyJet substrates?

Traces were written and dried at 55°C for 30 minutes. This was found to speed the drying of the conductor and to have no measurable effect on feature geometry or final conductivity when compared to traces dried at room temperature for over 24 hours. Higher drying temperatures could improve conductivity, but are not fully investigated because of the PolyJet material's low heat-deflection temperature.

Research Question 3: What are the adhesion characteristics between the conductive ink and PolyJet substrates?

Image-based contact angle measurements were gathered from deposited droplets and traces of conductive ink in both wet and dry states to determine adhesion characteristics between the ink and substrates. Additionally a scotch tape test was performed on the deposited features. Comparing the two PolyJet substrates, the contact angle of the conductive inks is observed to be larger when deposited on TangoBlack+ than on VeroWhite+, when using the same dispense parameters. This results in narrower, but taller, features on TangoBlack+ than on to VeroWhite+. It is also observed from contact angle measurements that the conductive ink exhibits a hydrophilic interaction with the

PolyJet substrates, which is an indicator of good adhesion as supported by the successfully scotch tape test.

Research Question 4: How does embedding and encapsulation effect conductivity of directly written conductors?

Samples were prepared with conductive ink deposited on PolyJet substrate surfaces as well as encapsulated with and without recessed channels for deposition—a total of 3 configurations. The measured geometries were used to design and dimension channels in PolyJet components for embedding and encapsulating conductors. The samples were dried according the procedure in RQ2 and trace resistances were measured. Fully encapsulated conductors exhibited lower conductivity than those deposited on the substrate surface. 50 mm long traces had average resistances of 1.36 Ohm on the surface and 26.2 Ohms when encapsulated.

By combining additive manufacturing, component embedding, and direct write processes, this work demonstrates the ability to create structurally integrated electrical interconnects and sensors. Using embedded strain and capacitance sensors, embedded electronics are shown to have many potential advantages over traditional assemblies including material reduction, assembly simplification, and direct manufacture.

6.2 Research Contributions

In summary, the main contributions of this work are:

- Identification of considerations for combining direct write and Additive Manufacturing technology.

These considerations are generalized to be applicable to any combination of direct write and additive manufacturing process. Future works may use this research to develop different hybridized systems of direct write and additive manufacturing tailored to specific research needs. These considerations are presented in Section 2.5 as well as in a peer-reviewed paper published in the 2013 International Solid Freeform Fabrication Symposium [51].

- The design and development of a direct write machine for dispensing conductive materials during the PolyJet build process.

This machine provides a platform for depositing different conductive materials during the PolyJet build process to analyze critical dispense parameters for conductive inks and how they behave on PolyJet substrates.

- Identification of important processing parameters for dispensing conductive materials and their impact on achievable resolution and conductivity.

This research provides the important parameters and metrics that should be analyzed when dispensing new conductive materials so as to understand the material's compatibility with PolyJet substrates including achievable feature size, drying considerations, adhesion, and conductivity.

- Analysis of drying, adhesion, and conductivity of DuPont ink on PolyJet substrates both on the surface and when encapsulated.

This analysis demonstrates the potential capabilities and limitations of using metal loaded conductive inks both on the surface of and fully embedded in PolyJet components. These limitations are presented in the following section.

6.3 Limitations and Future Work

The advantages of combining direct write and PolyJet are well documented through this thesis, however there also limitations to the process. There are still gaps in the parameterization of the direct write system, and better feature resolution and conductivity may still be possible yet. Moreover, PolyJet materials are not capable of withstanding the heat necessary for post process sintering that could dramatically improve the conductivity of the directly written features. Additionally, the insertion and removal of the direct write system makes multilayered conductors infeasible because of time and added labor.

Future work that might help circumvent these limitations includes, (i) further parameterization of the direct write system, (ii) exploration of alternative methods for sintering conductive materials on PolyJet substrates, and (iii) the development of a unified integration of Additive Manufacturing with conductive material deposition capabilities.

6.3.1 Further Parameterization and Improvement of the Direct Write System

The current iteration of the deposition machine is designed with the deposition toolhead orthogonal to the build tray at all times. As a result, the extrudate is under more shear stress than if the dispense tip were angled away from the deposition site. Analyzing different angles for dispensing could improve dispense characteristics and potentially enhance the minimum achievable feature size.

A better understanding is needed of the effects of the dispense tip offset from the surface. It is observed that due to imperfections in the lead screws, the offset distance was not always held constant. After setting the toolhead height and moving to a different area of the build tray, the height would need to be reset. The addition of linear shafts to constrain the deposition plane could improve the offset consistency over the entire build tray and improve performance. Further examination of the contact angle could also produce more consistent results over different substrates.

Moreover, regarding Research Question 4, there is further investigation required regarding the complete drying of encapsulated traces. Can traces be dried to a comparable conductivity as those traces on the surface before encapsulation? Longer drying times may also affect the PolyJet process. It is unclear how extended pausing times might affect PolyJet part quality or strength.

Because VeroWhite+ and TangoBlack+ can be digitally graded or mixed to create a composite mixture of the two, it is important to verify how the conductive materials behave on the digitally graded composites. It is possible to use the mixtures to define specific bead widths. For composite surfaces, contact angle is defined by Equation 6.1 where γ_1 and γ_2 are the proportions of each material in the composite, and θ_1 and θ_2 are their corresponding contact angles [40]. Therefore, any bead width between the averages of VeroWhite+ and TangoBlack+ should be achievable, as the individual contact angles have been measured.

$$\cos\theta = \gamma_1 \cos\theta_1 + \gamma_2 \cos\theta_2 \qquad \text{Equation 6.1}$$

6.3.2 High Temperature Processing of Conductive Materials

As explained in Chapter 2, post-deposition heating can improve conductivity and performance of the conductive inks but the temperatures required are beyond the glass transition temperatures of the PolyJet materials. Through our investigations, it is evident that PolyJet material can withstand some of these temperatures, although they may experience temporary softening when heated. A preliminary investigation shows that heating to 280°C will help to improve conductivity. However, at this temperature, the PolyJet substrate will discolor, which implies other potential changes to the material properties.

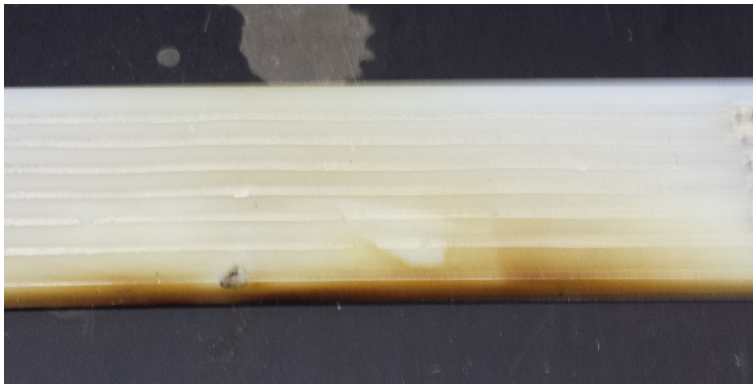

Figure 6.1: Discoloration of VeroWhite+ material after exposure to temperatures of 280°C

While not focused on AM, there has been interest in evolving sintering techniques to be compatible with low temperature substrates, specifically polymers. Perelaer and Schubert have investigated multiple localized methods for sintering directly written conductive traces [38]. They found that material can be locally sintered using laser or microwave radiation. Laser-based sintering still poses the risk of damaging a polymer substrate. This damage on a photopolymer substrate (fabricated by stereolithography) is characterized by Medina and coauthors [13]. Microwave radiation based sintering exhibited promising results; however, microwave conductors or antenna were required to absorb useful amounts of radiation, which is unpractical for volume processing. Another method for polymer compatible sintering is pulsed photonic curing. Pulsed photonic curing is interesting in the context of AM because it can heat metal traces to high temperatures without damaging the surrounding substrate. It is also a broadcast energy source so alignment to the traces is not necessary [52]. Preliminary work by Cormier suggests that the technology is safe for low temperature AM substrates [53].

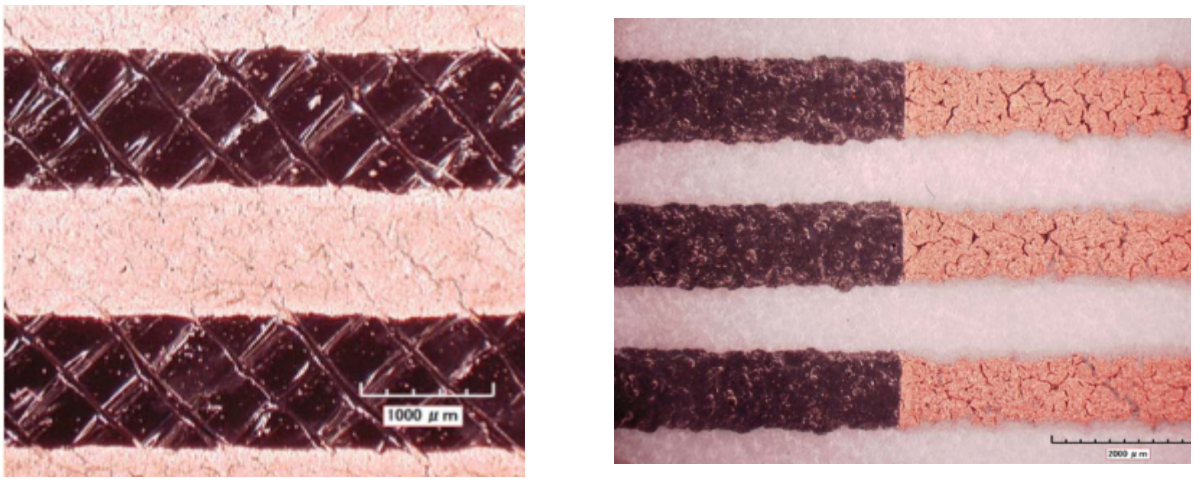

(a) (b)

Figure 6.2 – Photonic curing of copper on (a) FFF and (b) SLS substrates. (b) Also shows an intentionally uncured region in black used under fair use, 2013 [53]

Figure 6.2 shows examples of copper cured by photonic curing on both Fused Filament Fabrication and Laser Sintering manufactured substrates. The conductive materials for photonic curing can easily be deposited using inkjet technology, and the cured materials have shown conductivities of 10^9 S/m (greater than bulk conductivity of copper). The disadvantages of photonic curing are that the distance from the energy source is critical; therefore curing conductive inks is restricted to planar surfaces. Additionally, the thickness of the deposited ink is critical for curing and is restricted to relatively thin layer heights. Successful curing has not been demonstrated with thicknesses larger than 1-3 microns [52]. However, features this thin are possible with inkjet or Aerosol Jet direct write technologies.

6.3.3 Assessment of Aging Effects of Conductors under Various Environmental Conditions

Because directly written and encapsulated conductors are essentially inaccessible and non-serviceable after production, it is important to understand the effects of time on conductor performance. Temporal observations over a time period of years under various storage conditions is necessary. It is likely that temperature, humidity, and UV light exposure will affect the PolyJet structure and conductor's performance over time. While these effects may not

render the electronics non-functional, there may be a need to recalibrate embedded conductors over time.

6.3.4 Assessment of Conductive Material Distribution in the Cross-Section and Interface Interactions

During deposition in curing, it is uncertain of how particle density changes along the width of the conductors. It is possible that particle migration occurs to or from the center of the deposited trace. As a result the particle density may very across the cross-section. Scanning electron microscopy analysis of the cross-section can help reveal and variation in density. This variation is important because of conductivity. While this work has assessed the geometry of the deposited traces at an optical scale, it remains unclear how much of the cross-sectional geometry is comprised of conductive material.

Moreover, future work should provide an assessment of interface between the PolyJet substrate and conductive material. It is known that solvents commonly used for metal-loaded inks may chemically react with polymer materials. Therefore, there may be some chemical interaction at the material interface. Such an interaction could degrade the PolyJet material, but it may also said the adhesion of the two materials. Understanding how the solvent specifically reacts with PolyJet materials will help to further our understanding of this material interface.

6.3.5 Unified Integration of AM with Conductive Material Deposition Capabilities

While this thesis focuses on the hybridization of two distinct technologies, it is prudent to understand how these technologies could come together as a unified solution. An example of this is the carbon-filled FFF material developed by Leigh and coauthors [15]. Although not as conductive as the metal materials used in other works, the carbon material is processed through the AM technology's native material patterning system (extrusion), which allows the deposited conductive material to match the parameters of the structural components. An AM process that is capable of depositing both structural and conductive materials is ideal. But by matching the parameters of both direct write and AM systems, it is feasible to create a hybridized system that behaves more as a unified technology. It is possible that a conductive ink could be formulated to match the rheology of the PolyJet photopolymer resins such that it could be jetted using the native material deposition system. Since metal inks are preferred because of their high-

conductivity, a low temperature polymer compatible sintering process is desired to produce conductors comparable to those created by traditional circuit manufacturing technology. Sintering and deposition by the native material patterning system would also make multilayered interconnects feasible without dramatically increasing process time.

REFERENCES

[1] J. A. Palmer, D. Davis, B. D. Chavez, P. Gallegos, R. B. Wicker, and F. Medina, “Rapid Prototyping of High Density Circuitry,” Rapid Prototyping & Manufacturing no. 313, 2004.

[2] A. Kataria and D. W. Rosen, “Building around inserts: methods for fabricating complex devices in stereolithography,” Rapid Prototyping Journal, 2001.

[3] C. E. Folgar, L. N. Folgar, D. Cormier, and R. Hill, “Multifunctional material direct printing for laser sintering systems,” *Int. Solid Free. Fabr. Symp.* pp. 282–296, 2013.

[4] “Visualization of the working concept behind the strain gauge on a beam under exaggerated bending,” 2007. [Online]. Available: http://en.wikipedia.org/wiki/Strain_gauge. [Accessed: 02-Dec-2913].

[5] C. B. Williams, F. Mistree, and D. W. Rosen, “A Functional Classification Framework for the Conceptual Design of Additive Manufacturing Technologies,” *J. Mech. Des.*, vol. 133, no. 12, p. 121002, 2011.

[6] I. Gibson, D. W. Rosen, and B. Stucker, *Additive Manufacturing Technologies*. Boston, MA: Springer US, 2010.

[7] J. Stiltner, C. B. Williams, and A. Elliott, “A Method for Creating Actuated Joints Via Fiber Embedding in a Polyjet 3D Printing Process,” *Int. Solid Free. Fabr. Symp.* pp. 1–10, 2011.

[8] C. B. Williams, “Embedded Flexible Control Surfaces,” pp. 1–15, 2011.

[9] A. Lopes, M. Navarrete, F. Medina, J. Palmer, E. Macdonald, and R. Wicker, “Expanding Rapid Prototyping for Electronic Systems Integration of Arbitrary Form,” *Int. Solid Free. Fabr. Symp.*, pp. 644–655, 2006.

[10] L. Mortara, J. Hughes, P. S. Ramsundar, F. Livesey, and D. R. Probert, “Proposed classification scheme for direct writing technologies,” *Rapid Prototyp. J.*, vol. 15, no. 4, pp. 299–309, 2009.

[11] K. K. B. Hon, L. Li, and I. M. Hutchings, “Direct writing technology—Advances and developments,” *CIRP Ann. - Manuf. Technol.*, vol. 57, no. 2, pp. 601–620, Jan. 2008.

[12] K. H. Church, C. Fore, and T. Feeley, “Commercial Applications and Review for Direct Write Technologies,” *MRS Proc.*, vol. 624, p. 3, Feb. 2011.

[13] F. Medina, A. Lopes, A. Inamdar, R. Hennessey, J. Palmer, B. Chavez, D. Davis, P. Gallegos, and R. Wicker, “Hybrid Manufacturing: Integrating Direct Write and Stereolithography,” *Int. Solid Free. Fabr. Symp.*, 2005.

[14] D. Periard, E. Malone, and H. Lipson, “Printing Embedded Circuits,” *Int. Solid Free. Fabr. Symp.*, pp. 503–512, 2007.

[15] S. J. Leigh, R. J. Bradley, C. P. Purssell, D. R. Billson, and D. a. Hutchins, “A Simple, Low-Cost Conductive Composite Material for 3D Printing of Electronic Sensors,” *PLoS One*, vol. 7, no. 11, p. e49365, Nov. 2012.

[16] K. Miyasaka, K. Watanabe, E. Jojima, H. Aida, M. Sumita, and K. Ishikawa, “Electrical conductivity of carbon-polymer composites as a function of carbon content,” *J. Mater. Sci.*, vol. 17, no. 6, pp. 1610–1616, Jun. 1982.

[17] K. Teng and R. Vest, “Liquid Ink Jet Printing with MOD Inks for Hybrid Microcircuits,” *IEEE Trans. Components, Hybrids, Manuf. Technol.*, vol. 10, no. 4, pp. 545–549, Dec. 1987.

[18] Y. Zhang, C. Liu, and D. Whalley, “Direct-write techniques for maskless production of microelectronics: A review of current state-of-the-art technologies,” *2009 Int. Conf. Electron. Packag. Technol. High Density Packag.*, pp. 497–503, Aug. 2009.

[19] B Li, P. A. Clark, and K. H. Church, “Robust Direct-Write Dispensing Tool and Solutions for Micro/Meso-Scale Manufacturing and Packaging,” 2007. [Online]. Available: http://www.nscrypt.com/.

[20] R. Wicker, F. Medina, and C. Elkins, “Multiple material micro-fabrication: extending stereolithography to tissue engineering and other novel applications,” *Proc. 15th …*, pp. 754–764, 2004.

[21] F. Medina, A. V Inamdar, R. Hennessey, E. Paso, J. A. Palmer, and B. D. Chavez, “Integrating Multiple Rapid Manufacturing Technologies for Developing Advanced Customized Functional Devices,” in *Rapid Prototyping*, 2005.

[22] “MicroFab Technote 99-01: Background on Ink-Jet Technology,” 1999. [Online]. Available: http://www.microfab.com/.

[23] E. Tekin, P. J. Smith, and U. S. Schubert, “Inkjet printing as a deposition and patterning tool for polymers and inorganic particles,” *Soft Matter*, vol. 4, no. 4, p. 703, 2008.

[24] S. Thomas, H. Temp, and L. Temp, “Electronics Manufacturing by Inkjet Printing,” in *IPC Printed Circuit Expo, APEX & Designer Summit*.

[25] S. B. Walker and J. a Lewis, “Reactive silver inks for patterning high-conductivity features at mild temperatures.,” *J. Am. Chem. Soc.*, vol. 134, no. 3, pp. 1419–21, Jan. 2012.

[26] C. Goth, S. Putzo, and J. Franke, “Aerosol Jet printing on rapid prototyping materials for fine pitch electronic applications,” *2011 IEEE 61st Electron. Components Technol. Conf.*, pp. 1211–1216, May 2011.

[27] Optomec, “Optomec Aerosol Jet 300 Series Data Sheet.” [Online]. Available: www.optomec.com.

[28] Optomec, “Aerosol Jet Print Engine Datasheet,” 2013.

[29] C. J. Robinson, B. Stucker, A. J. Lopes, R. Wicker, and J. Palmer, “Integration of Direct-Write (DW) and Ultrasonic Consolidation (UC),” *Int. Solid Free. Fabr. Symp.*, 2006.

[30] J. J. Casanova, J. A. Taylor, and J. Lin, “Design of a 3-D fractal heatsink antenna,” *IEEE Antennas Wirel. Propagattion Lett.*, vol. 9, pp. 1061–1064, 2010.

[31] E. Malone, M. Berry, and H. Lipson, “Freeform fabrication and characterization of Zn-air batteries,” *Rapid Prototyp. J.*, vol. 14, no. 3, pp. 128–140, 2008.

[32] K. Sun, T.-S. Wei, B. Y. Ahn, J. Y. Seo, S. J. Dillon, and J. a. Lewis, “3D Printing of Interdigitated Li-Ion Microbattery Architectures,” *Adv. Mater.*, Jun. 2013.

[33] S. Castillo, D. Muse, F. Medina, E. Macdonald, and R. Wicker, “Electronics Integration in Conformal Substrates Fabricated with Additive Layered Manufacturing,” *Int. Solid Free. Fabr. Symp.*, pp. 730–737, 2009.

[34] R. I. Olivas, “Conformal electronics packaging through additive manufacturing and micro-dispensing,” University of Texas at El Paso, 2011.

[35] Stratasys, “PolyJet Materials Data Sheet Materials Simulating Engineering Plastics.” 2013.

[36] G. L. Allen, R. a. Bayles, W. W. Gile, and W. a. Jesser, “Small particle melting of pure metals,” *Thin Solid Films*, vol. 144, no. 2, pp. 297–308, Nov. 1986.

[37] A. McNaught and A. Wilkinson, *Compendium of Chemical Terminology*, 2nd ed. Malden, MA: Blackwell Science, 1997.

[38] J. Perelaer, U. S. Schubert, and F. Jena, “Inkjet Printing and Alternative Sintering of Narrow Conductive Tracks on Flexible Substrates for Plastic Electronic Applications,” in in *Radio Frequency Identification Fundamentals and Applications, Design Methods and Solutions*, C. Turcu, Ed. InTech, 2010, pp. 265–286.

[39] A. Lopes, E. MacDonald, and R. B. Wicker, “Integrating stereolithography and direct print technologies for 3D structural electronics fabrication,” *Rapid Prototyp. J.*, vol. 18, no. 2, pp. 129–143, 2012.

[40] K. L. Mittal, *Advances in contact angle, wettability, and adhesion*. Hoboken: Wiley Scrivener Pub, 2013.

[41] W. Cheng, P. F. Dunn, and R. M. Brach, “Surface Roughness Effects on Microparticle Adhesion Modeling of Adhesion for Smooth Surfaces,” *J. Adhes.*, pp. 929–965, 2002.

[42] J. S. Mijovic and J. a. Koutsky, “Etching of Polymeric Surfaces: A Review,” *Polym. Plast. Technol. Eng.*, vol. 9, no. 2, pp. 139–179, Jan. 1977.

[43] E. M. Liston, L. Martinu, and M. R. Wertheimer, “Plasma surface modification of polymers for improved adhesion: a critial review,” *J. Adhes. Sci. Technol.*, vol. 7, no. 10, 1993.

[44] A. Breyfogle and K. Vartanian, “Capability Assessment of Combining 3D Printing (FDM) and Printed Electronics (Aerosol Jet) Processes to Create Fully Printed Functionalized Devices,” *Rapid Prototyp.*, 2013.

[45] J. J. Benbow and E. W. Oxley, “The Extrusion Mechanics Of Pastes-The Influence Of Paste Formulation Extrusion Parameters,” vol. 42, no. 1967, 1987.

[46] T. D. Sheet and P. Description, “DuPont Conductive Silver Compositions for General Purpose Air-Dry Applications,” pp. 1–6.

[47] HIROX, “Digital Microscope KH-7700 Information Page,” 2013. [Online]. Available: http://www.hirox-usa.com/products/microscope/kh7700_01.html. [Accessed: 09-Dec-2013].

[48] J. R. Huntsberger, “The Relationship between Wetting and Adhesion,” pp. 180–188, 1964.

[49] Z. Wang, J. Li, G. Hang, and Y. Wang, “A Flexible Hingeless Control Surface Inspired by Aquatic Animals,” *J. Bionic Eng.*, vol. 7, no. 4, pp. 364–374, Dec. 2010.

[50] N. Meisel, A. Elliott, and C. B. Williams, “A procedure for creating actuated joints via embedding shape memory alloys in PolyJet 3D printing,” *J. Intell. Mater. Syst. Struct.*

[51] K. B. Perez and C. B. Williams, “Combining Additive Manufacturing and Direct Write for Integrated Electronics – A Review,” *Int. Solid Free. Fabr. Symp.*, pp. 962–979, 13AD.

[52] K. A. Schroder, S. C. Mccool, and W. F. Furlan, “Broadcast Photonic Curing of Metallic Nanoparticle Films Basic Process Research and Development System,” in *The Nanotechnology Conference and Trade Show*, 2006, vol. 3, no. 512, pp. 198–201.

[53] D. Cormier and S. Farnsworth, “Pulsed Photonic Curing of Printed Functional Materials,” in *Rapid Prototyping*, 2013.

APPENDIX A: RAW DATA FROM RQ1

This section contains a table of exhaustive raw data for the experiment discussed in Section 4.1.

Table A.1: Raw data for line width measurements in Research Question 1

Text

Trial Number	Dispensing Pressure [psi]	PolyJet Substrate	Toolhead Speed [mm/min]	Sample 1	Sample 2	Sample 3	Sample 4	Average	Std. Dev.
1	4.5	VeroWhite+	1000	1.235	1.307	1.381	1.354	1.319	0.055
2	4.5	VeroWhite+	2000	1.142	1.022	1.046	1.070	1.070	0.045
3	4.5	VeroWhite+	3000	0.880	0.831	0.926	0.879	0.879	0.034
4	4.5	TangoBlack+	1000	1.022	0.974	0.855	0.975	0.957	0.062
5	4.5	TangoBlack+	2000	0.784	0.808	0.879	0.784	0.814	0.039
6	4.5	TangoBlack+	3000	0.831	0.713	0.642	0.693	0.720	0.069
7	5.5	VeroWhite+	1000	1.689	1.540	1.615	1.639	1.621	0.054
8	5.5	VeroWhite+	2000	1.164	1.021	1.378	1.259	1.206	0.131
9	5.5	VeroWhite+	3000	1.045	1.425	1.094	1.190	1.189	0.146
10	5.5	TangoBlack+	1000	1.164	1.235	1.140	1.259	1.200	0.049
11	5.5	TangoBlack+	2000	0.950	0.926	0.926	0.808	0.903	0.055
12	5.5	TangoBlack+	3000	0.736	0.831	1.021	0.760	0.837	0.112